Advanced Engineering Materials

ADVANCED ENGINEERING MATERIALS
www.aem-journal.com

REVIEW OPEN ACCESS

Light-Assisted 3D Printing Techniques and Photocrosslinking Strategies: Recent Advances in Musculoskeletal Tissue Engineering

Meagan Morgan[1] | Bin Zhang[2] | Roger Narayan[1]

[1]Lampe Joint Department of Biomedical Engineering, University of North Carolina and North Carolina State University, Raleigh, North Carolina, USA | [2]Department of Mechanical and Aerospace Engineering, Brunel University London, London, UK

Correspondence: Roger Narayan (roger_narayan@ncsu.edu)

Received: 28 August 2025 | **Revised:** 11 May 2026 | **Accepted:** 13 June 2026

Keywords: biomaterials | bioprinting | musculoskeletal | stereolithography | tissue engineering

ABSTRACT

Musculoskeletal (MSK) disorders represent a significant global health challenge that affects over 1.7 billion people, leading to physical disability as well as reduced mental health and socioeconomic well-being. Despite their high prevalence, MSK diseases remain severely underfunded compared to other global health priorities. Tissue engineering and regenerative medicine (TERM) can utilize light-based 3D bioprinting and photocrosslinking methods for the treatment and study of MSK conditions. Light-based bioprinting techniques, such as digital light processing and stereolithography, enable the creation of high-resolution scaffolds that mimic the complex, highly organized structure of MSK tissues, while photocrosslinking methods can be applied more broadly across nonlight-based techniques to improve ink or scaffold stability. These technologies hold the potential for advancing MSK therapies; however, the need for specialized photocurable materials, cytotoxicity concerns, and mechanical limitations of printed constructs remains. This systematic review addresses current gaps and trends in light-assisted 3D printing for MSK applications, examines the most frequently used biomaterials and cell types over the past 5 years, and highlights future research directions to advance TERM for MSK repair and regeneration.

1 | Introduction

Musculoskeletal (MSK) health is the foremost cause of disability worldwide, affecting nearly 1.7 billion individuals [1]. In the United States alone, an average of one in three people suffers from MSK disorders. These disorders involve a wide range of impacted tissues such as bone, skeletal muscle, connective tissue, and whole-joint anatomy. Common MSK diseases include chronic pain caused by osteoarthritis or injuries, osteoporosis, and inflammatory diseases such as rheumatoid arthritis. These conditions are directly linked to long-term loss of mobility and pain, and have broader implications associated with changes to mental health and socioeconomic consequences [1, 2]. Despite their widespread presence, MSK disorders are the most underfunded among similar global health challenges [3].

In response to these challenges, tissue engineering and regenerative medicine (TERM) offer a promising approach for treating MSK conditions. The combination of advanced biomaterials and cell sources has been used to develop tissue scaffolds for clinical implantation or as benchtop modeling tools to improve treatment and prevention strategies of MSK diseases [4, 5]. Pioneered by Charles W. Hull with the first stereolithographic printer [6], 3D printing technologies offer automated precision in the fabrication of complex scaffold geometries, an advancement that has received significant attention in TERM research. Since 1987, various techniques have been commercialized, such as extrusion, inkjet, digital light processing, two-photon polymerization, selective laser sintering, and volumetric additive manufacturing [5, 7].

The use of light to initiate polymerization and solidify a structure serves as the basis of light-based 3D printing. The primary mechanism in light-based 3D printing, known as photocrosslinking, is controlled by selective light exposure, enabling design flexibility. Photocrosslinking offers rapid post-processing of 3D-printed parts. In this review, the combination of light-based 3D printing and 3D printing plus photocrosslinking will be termed light-assisted printing techniques. Despite the benefits of these approaches, several challenges remain. Light-assisted 3D printing is associated with several limitations, including the requirement for photocurable precursor materials, the high cost of light-based 3D printers, and the cytotoxic effects of uncontrolled light exposure [8, 9].

Three key questions are proposed by this review to address the future use of light-assisted 3D printing techniques for musculoskeletal TERM applications:

1. What are the current gaps in light-assisted 3D printing of musculoskeletal tissues?
2. What are the current trends in light-assisted 3D printing of musculoskeletal tissues?
3. What are the current challenges associated with light-assisted 3D printing of musculoskeletal tissues?

By addressing these questions, this review will help identify frequently used methods, biomaterials, and target tissue types, while closing the gap in existing review articles that separately discuss light-assisted 3D printing and MSK tissue engineering but not their distinct overlap. The combination of these goals will hopefully stimulate future investigation within these fields, particularly involving underinvestigated target tissues such as skeletal muscle, tendon, ligament, and synovial membrane. Systematic retrieval of articles was conducted from two databases using the terms "light bioprinting" and a specified MSK tissue type (e.g., "bone" and "cartilage"). The included research articles utilized a form of light-assisted 3D printing in their methods, focused on an MSK tissue, and were published within the last 5 years. This review compiles the printing methods, biomaterials, cell types, and assessment tools from the selected studies to formulate conclusions on current scaffold limitations for clinical use and commercialization.

2 | Light-Based 3D Bioprinting Techniques

2.1 | Stereolithography

Stereolithography (SLA) uses a UV laser to photopolymerize liquid resin onto a build plate in a layer-by-layer manner until a final 3D object is constructed [9]. This process utilizes controlled UV light to achieve detailed structures based on computer-aided design (CAD) inputs [10]. There are two setups, either a top-down or a bottom-up setup, depending on the location of the laser with respect to the build plate. Typically, the bottom-up, or inverted SLA, setup is used as it is more economical, requiring a lower volume of resin. The term "stereolithography" also refers to the file format (.stl) used in 3D printing to represent 3D models. SLA offers several advantages, particularly in creating intricate structures, as further detailed in Table 1 [9, 18]. For example, SLA allows for the printing of fine-scale features necessary for mimicking the cellular architecture of human tissues, making it an appropriate technique for use in tissue scaffold fabrication [19, 20].

2.2 | Digital Light Processing

A type of SLA printing, digital light processing (DLP), uses light to cure a pre-determined pattern within a vat of photocurable resin. Unlike SLA techniques, DLP printing uses the projection of UV light to cure an entire layer of material at once. This process is possible due to the use of a digital micromirror device (DMD) chip, which uses reflective micro-scale mirrors to direct light into individual pixels of an image, which is often generated using CAD software. The pixel size determines the printer resolution, which can be as small as 1 μm. This approach can build structures relatively quickly since it involves curing an entire layer of material at once. Several parameter selections are necessary for optimized matching of the features between the 3D-printed structure and the 3D model, such as light intensity, layer height, and curing time; it should be noted that resin selection also plays a large role in determining these parameters [4, 21].

2.3 | Two-Photon Polymerization

Two-photon polymerization (TPP) is a photopolymerization technique with the highest resolution, around 100 nm to date. Several parameters, including the laser power, exposure time, and photoinitiator choice, determine the resolution. TPP utilizes an ultrafast laser to pattern photocurable resin in a pattern that is defined using a 3D model [7, 22]. The most common materials used in TPP are negative-tone resins, which polymerize in the presence of two or more absorbed photons. TPP can also utilize positive-tone resins, which degrade the patterned material for subsequent dissolution using a common solvent, leaving the negative structure as the intact final structure [22]. While TPP methods are capable of producing complex features, they are limited to small constructs due to the slow print speed. Additionally, TPP is only compatible with materials that can be characterized as water-soluble and include an initiator that is compatible with multiphoton absorption [7].

2.4 | Other Light-Based 3D Bioprinting and Photocrosslinking Techniques

In addition to the most common light-based 3D bioprinting techniques mentioned above, several alternative photocrosslinking methods are available. Extrusion-based printing is not a light-based 3D printing strategy; however, it is commonly used in conjunction with photocrosslinking methods. Scaffolds are constructed by extruding filaments of ink into connected and layered strands; an external photocuring unit is used to solidify scaffold geometries by polymerizing the bioink during or after printing [5]. This method requires a viscous, shear-thinning ink for cell protection, but it is relatively low in cost compared to light-based methods [8]. Laser-induced forward transfer (LIFT) is a contactless method that uses laser pulses to propel bioink onto a substrate; this approach offers the potential for single-cell deposition, making it useful for creating cell-laden structures [5, 8, 15]. An alternative single-cell deposition technique was recently described that involves contact photolithography using PDMS cell imprints [23]. Volumetric

TABLE 1 | Summary of the advantages and limitations of light-assisted printing strategies.

Technique	Advantages	Limitations	Ref.
DLP	• High resolution (15–30 μm) • Moderate speed • High ink cell density (10^8 mL^{-1}) • Moderate interface complexity • Nozzle-free method	• Moderate print size • High material quantity • Low viscosity materials • Transparent, photosensitive materials	[5, 11–14]
SLA	• High resolution (2–100 μm) • High ink cell density (10^8 mL^{-1}) • Moderate interface complexity • Nozzle-free method	• Slow/moderate speed • Moderate print size • High material quantity • Low viscosity materials • Transparent, photosensitive materials	[5, 12–15]
TPP	• Very high resolution (100 nm–1 μm) • Moderate material quantity • Moderate interface complexity • Nozzle-free method	• Very slow speed • Small print size • Low viscosity materials • Transparent, photosensitive materials	[12, 13]
LIFT	• Very high resolution (1–10 μm) • Moderate speed • Low material quantity • Moderate interface complexity • Nozzle-free method	• Small print size • Low ink cell density (10^6 mL^{-1}) • Low viscosity materials • Possible 2^{nd} crosslinking mechanism required	[5, 8, 14–16]
VAM	• High resolution (50–200 μm) • Fast speed • Moderate material quantity • Layerless, nozzle-free method	• Small print size • Moderate/high viscosity materials • Moderate/high interface complexity • Light scattering from cell-laden materials	[12, 17]
Extrusion	• Moderate resolution (100–500 μm) • Large print size • Low material quantity • High ink cell density (10^8–10^9 mL^{-1}) • Low interface complexity	• Slow speed • High viscosity materials • Shear-thinning materials • Nozzle-based method	[5, 8, 12, 14–16]

additive manufacturing (VAM) involves linear or tomographic approaches; both utilize multidirectional light projections for rapid 3D printing at high resolution (25–80 μm) [21, 24]. These photo-based techniques offer diverse approaches for TERM applications. Each approach is associated with unique advantages and disadvantages in terms of resolution, speed, and biocompatibility.

3 | Biomaterials

Resin-based biomaterials are often used in light-based bioprinting and photocrosslinking strategies. These biomaterials typically consist of several components, such as the polymer precursor, photoinitiator, absorber, additive, and filler. These resin elements are detailed in Figure 1.

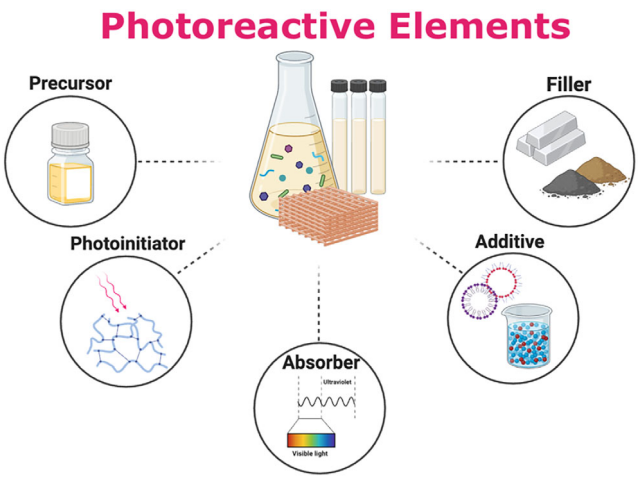

FIGURE 1 | A graphical representation of potential photocurable resin components. Created using Biorender.

3.1 | Biocompatible Polymers

The choice of polymer resin in light-assisted 3D bioprinting is an important decision since the choice of the polymer resin determines the properties of the biocompatible scaffold, including its support of cell growth and tissue formation. There is a wide variety of available precursors. Polymer resin selection should be guided by the compatibility requirements of the target tissue as well as the intended print quality. For the former goal, criteria must be met in terms of biocompatibility and mechanical stability. For the latter goal, precursors must have the capability to undergo polymerization under light exposure. Natural polymers such as silk fibroin, gelatin, alginate, collagen, hyaluronic acid, and their hybrid formulations are frequently used due to their

excellent biocompatibility. Most precursors must undergo modifications such as thiolation or methacrylation to enable high-resolution photocuring. One downside to these polymers is their lack of mechanical strength relative to native MSK tissues. For example, gelatin is a denatured form of collagen that has lost its triple helix backbone and exhibits reduced mechanical properties. Gelatin methacryloyl (gelMA) is a very popular ink for photopolymerization since the methacrylate group allows the polymer to undergo free-radical chain reactions [7, 25].

Further precursor modifications can be made to improve the mechanical and biological properties of the ink. As shown in Figure 2, the modification process used with the polymer may affect its composition and biological functionality. The use of a higher precursor concentration has been shown to significantly increase the hydrogel stiffness, but it is associated with challenges related to ink homogeneity [27, 28]. The use of a lower precursor concentration allows for lower crosslink densities, which improves nutrient transport between encapsulated cells [29]. An improvement in nutrient transport at higher precursor concentrations can be obtained by preparing a hydrogel with a high swelling ratio [30, 31]. Beyond precursor concentration, studies have shown that the temperature at which a hydrogel precursor cures can impact its resulting stiffness; lower temperatures, those close to physical gelation, produce stiffer hydrogels. Additionally, exposure to air can result in oxygen inhibition of the crosslinking reaction, limiting the overall stiffness [32].

A method to further enhance biocompatibility, mechanical properties, and functionality of printed constructs is through composite hydrogel systems. One of the most promising copolymers is decellularized extracellular matrix (dECM), which retains the native structural and biochemical cues of tissues. The material and environment support cell attachment, growth, and differentiation. dECM-based inks are often used to improve the tissue-specificity of bioprinted scaffolds [33, 34]. Other polymers such as hyaluronic acid, collagen, and alginate are used to enhance cell adhesion or improve the rheological properties of ink for 3D printing and cell differentiation [4, 35]. By incorporating copolymers, photocurable inks are tailored to the desired mechanical and biological properties of various MSK tissues. For example, the addition of acrylamide to a gelMA/HAMA bioink increased its compressive resistance, swelling ratio, and slowed its degradation rate [36]. There are a variety of polymer combinations to be considered for TERM resins; nevertheless, a balance between functionality and simplicity is best when considering reproducibility, availability of resources, and translation to clinical use.

3.2 | Photoinitiators

Photoinitiators are important components in light-assisted 3D bioprinting as they enable the polymerization of photocurable materials in response to controlled light exposure. These molecules are excited by specific wavelengths, typically in the UV to visible light spectrum, and trigger chain polymerization via the generation of free radicals or ionic species (Figure 3A) [21]. The functionality of photoinitiators is important for achieving functional TERM scaffolds since their effectiveness directly impacts the resolution, mechanical properties, and other functional attributes of a printed scaffold. Moreover, appropriate photoinitiator selection is key for modifying print factors such as polymerization speed, depth of cure, and cytotoxicity [11]. Irgacure 2959 (2-hydroxy-4′-(2-hydroxyethoxy)-2-methylpropiophenone) is a widely used photoinitiator in UV-based 3D printing. This photoinitiator exhibits its highest efficiency at a wavelength of 365 nm [37]. It is commonly used in 3D printing due to its rapid cure response and ability to produce high-quality, structurally stable printed constructs. However, another consideration is the impact of the photoinitiator on cell toxicity during printing. The use of shorter light wavelengths can reduce cell viability and growth post-printing, limiting the use of UV-based bioprinting in sensitive biological environments [5, 21, 35]. This limitation has resulted in an increased interest in visible-light-based 3D printing, which uses photoinitiators activated at less biologically harmful wavelengths (typically around 405 nm) [37]. Common photoinitiators in this category include lithium phenyl-2,4,6-trimethylbenzoylphosphinate (LAP), ruthenium (Ru)/sodium persulfate (SPS), and 2,4,6-trimethylbenzoyldiphenyl phosphine oxide (TPO). Each of these photoinitiators is known for its low cytotoxicity and high printing efficiency [35, 38, 39]. Researchers have investigated alternative photoinitiators such as phenylbis(2,4,6-trimethylbenzoyl)phosphine oxide (BAPO), Eosin Y, and riboflavin; however, the biocompatibility of these photoinitiators with musculoskeletal tissues has not yet been fully established [7, 21].

Similar to precursor considerations, the choice of crosslinker can affect overall ink performance due to the various activation mechanisms. Ru/SPS, for example, can crosslink a dual

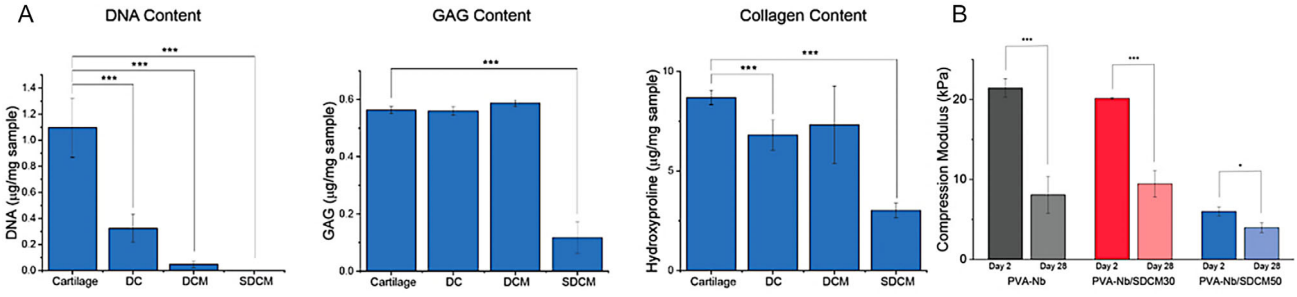

FIGURE 2 | Changes in ink due to preparation and polymer concentration. (A) Setayeshmehr et al. demonstrated changes in biomolecule content during polymer preparation and (B) mechanical strength from polymer concentration. *DC = devitalized cartilage, DCM decellularized cartilage matrix, SDCM = solubilized DCM. Means ± SD; ***$p < 0.001$. Reproduced under terms of the CC-BY license [26]. 2021 by the Authors, published by MDPI.

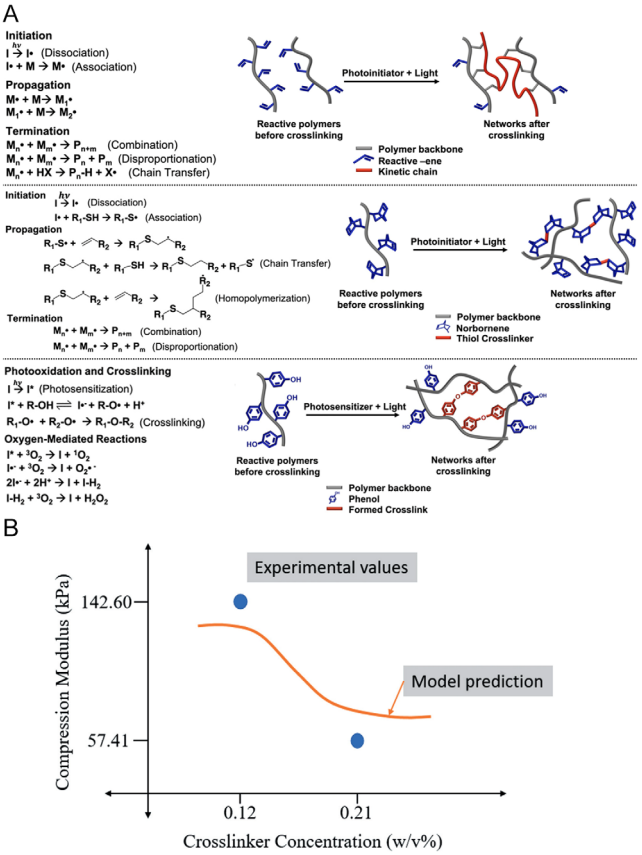

FIGURE 3 | Choice of photoinitiator impacts crosslinking mechanism and bioink properties. (A) General mechanisms for photocrosslinking resins via free-radical chain polymerization (top), radical-mediated thiolene crosslinking (middle), and photomediated redox reactions (bottom). Adapted with permission [37]. 2024, American Chemical Society. (B) Graph demonstrating the difficulty in modeling significant changes in compression modulus under varying photoinitiator concentration when other parameters (gelMA concentration, light intensity, and exposure time) are kept constant. Reproduced under terms of the CC-BY license [27]. 2024 by the Authors, published by IJB.

functionalized polymer via simultaneous chain growth polymerization and di-tyramine bonding, which is not achievable using I2959 or LAP alone [38]. Furthermore, the concentration of the photoinitiator can affect scaffold printability, cytotoxicity, and the resulting mechanical properties (Figure 3B). This includes cellular disruption from the light activation or chemical crosslinking by-products [27, 35, 38].

The development and optimization of these photoinitiators are critical for advancing this field. The balance between photopolymerization efficiency and biocompatibility is key for creating tissue scaffolds. Ongoing research into photoinitiator chemistry should focus on improving their efficiency, reducing potential harm to cells, and expanding the range of printable biomaterials for TERM applications.

3.3 | Additives

Absorbers can be added to photocurable resins to control the photopolymerization process. These agents manage light exposure by reducing penetration depth and preventing unwanted side effects, such as excessive curing, an important step toward feature retention and successful undercut geometry. Similar to photoinitiators, absorbers only work for specific light wavelengths. Absorbers can also prevent premature curing during print set-up [40, 41]. Common UV absorbers include phenol red, tartrazine, and benzophenone-9 (R1800) [40, 42, 43]. The choice and concentration of absorbers in the resin formula must be optimized for the best print result since these materials exhibit a reported dose-dependent cytotoxicity [41].

Fillers are metal, ceramic, or composite particles added to resins to enhance their performance through biological, mechanical, thermal, or electrical properties. Common fillers include inorganic materials such as hydroxyapatite particles (HAp) and beta-tricalcium phosphate (β-TCP); these bioactive ceramics are used primarily in bone tissue engineering due to their ability to support osteointegration and mimic the mineral content of native bone [39, 40, 44, 45]. These fillers not only provide structural stability but also promote cellular interactions that are essential for tissue regeneration. The choice to add other fillers depends on the desired properties of the bioprinted scaffold, such as flexibility, strength, degradation rate, or bioactivity. As such, fillers are an important component for tailoring photocurable inks that are used in bioprinting; however, due to printing mechanisms, it is important that the filler particles are smaller than the designated layer heights.

Akin to fillers, other additives are utilized for modifying ink behavior; however, only properties specific to printability are considered. High volume of filler in resin can produce highly viscous slurries, which impact ink flow and platform movement during printing. Diluents, stabilizers, and dispersants can be added to reduce viscosity, increase homogeneity, or prevent agglomeration and sedimentation of particles. Additive examples include xanthan gum, nanofibrillated cellulose, DISPERBYK (an alkylolammonium salt solution of a polycarboxylic acid polymer), coupling agent KH560, and oleic acid [39, 40, 46].

4 | Applications in Musculoskeletal Tissues

4.1 | Skeletal Muscle

The most abundant tissue in the body is skeletal muscle. This tissue type is responsible for several physiological tasks, including mechanical support, balance, organ protection, voluntary movement control, and storage for intracellular ions, as well as 80% of the water supply of the body [2, 47]. This highly organized tissue starts as muscle progenitor cells until differentiating and maturing into hundreds of muscle fibers that comprise a single muscle [47]. These fibers are made from fused myoblasts known as myotubes, which form sarcomeres. These complexes of actin and myosin proteins are responsible for muscle shortening and contractions. The striated appearance of skeletal muscle tissue arises from myofilaments that are formed from these myotubes. The complexity of replicating these tissues only increases when examining the fiber type based on its performance. Type I consists of slow-twitch fibers, which use aerobic metabolism to resist fatigue. Fast-twitch fibers that use anaerobic activity and

exhibit variable fatigue resistance make up Type II [2]. There are several challenges to address when engineering skeletal muscle tissue due to the complex features associated with this tissue type.

On a small scale, skeletal muscle tissue has an intrinsic ability to regenerate after injury. Satellite cells line each fiber, awaiting activation via detected myofiber damage to trigger cell proliferation for repair and replacement [48]. Individuals suffering from orthopedic trauma, surgical excision, or degenerative muscular disease commonly face an injury known as volumetric muscle loss (VML) [47]. VML defects represent a 20% loss of tissue, leading to long-term fibrosis, tissue scarring, and chronic loss of limb function [49]. Due to a lack of conventional treatment options, VMLs are commonly studied for tissue engineering applications in vivo alongside drug screening platforms in vitro.

Although few studies that target this clinical need utilize light-based bioprinting techniques, several studies that utilize photocrosslinking methodologies have been published (Table 2). Frías-Sánchez et al. used a technique termed chaotic 2D printing, in which UV light exposure cured bioink injections within controlled surface flows, creating uniform gelMA fibers ranging from 16.8 to 386.4 μm in diameter and 2.68–152.2 mm in length based on flow parameters. These fibers were able to maintain viable myoblasts for 28 days. The technique subjected the bioink to a high amount of shear stress, resulting in low initial cell viability; however, all groups recovered by the second week of culture. Although the mechanism was unclear, the addition of embedded turnip mosaic virus within the fibers increased cell attachment, and these fibers showed improved viability by the fourth week compared to pure gelMA fibers. Due to the design of these cell scaffolds, cell-to-fibrillar alignment was induced, and microstructure and striation patterns similar to those of native tissue were observed [62]. While gelMA is a popular choice in tissue engineering, modifications can be made to improve the performance of the material, as seen with the addition of alginate (Figure 3). GelMA combined with 8% alginate was shown to improve cell viability after culture for 7 days. More specifically, when the ink was dual crosslinked, initially with calcium chloride and followed by UV exposure, cell growth increased and promoted myotube formation compared to 0% and 6% alginate additions. The authors showed how culture conditions (e.g., under electrical stimulation) can increase the metabolic performance of the gelMA scaffolds. The limitations of measuring visual contraction prevented the assessment of gelMA-alginate constructs for comparison purposes [65].

As an alternative to developing novel inks, there are commercial bioink options compatible with skeletal muscle tissue, as shown by Ronzoni et al. Their study assessed the proliferation, viability, and differentiation profiles of murine myoblasts within three commercially available inks, two of which used photopolymerization to crosslink 20 mm fibers with 0.35 mm diameter. The best results were obtained from nanofibrillated cellulose/alginate/fibrinogen hydrogel (CELLINK FIBRIN), in comparison to a gelatin/alginate hydrogel (CELLINK GelMA A) and xanthan gum/fibrinogen hydrogel (CELLINK GelXA FIBRIN), where myotubes were shown to form after day 21–28 using CELLINK FIBRIN. It is unclear whether these results are affected by UV crosslinking or whether the differences stem from compositional differences among nano-fibrillated cellulose, alginate, and fibrinogen that is crosslinked with calcium chloride and thrombin [64].

Another study using light-assisted printing assessed the potential of in situ applications of 3D printing. Intravital 3D printing, a bioorthogonal two-photon cycloaddition and crosslinking approach, was used to crosslink bioink variations of porcine gelatin, PEG, and Matrigel within the skin, skeletal muscle, and brain tissues of living mice. The authors were able to print across the epimysium using gelatin laden with primary muscle cells and primary fibroblasts. Parallelepiped-shaped constructs gave the cells a distinct orientation compared to the nonirradiated injections. Furthermore, only this group of mice exhibited elongated bundles of cells containing myosin heavy chain and striated cytoskeleton, suggesting the authors were able to use this technique and bioink to support de novo muscle development in situ while achieving a range of Young's moduli able to match that of native tissue (1 – 20 kPa) [63].

All the previously described studies have used a denatured form of collagen called gelatin, which is derived from porcine skin. Sanz et al. considered an alternative to gelatin; they evaluated the performance of murine myoblasts and neural cells in methacrylated fish collagen, and commercially available bovine collagen was used for comparison purposes in their study. Coaxially printed neural and skeletal muscle cells within this ink produced a 10 × 10 × 0.6 mm in vitro model for neuromuscular junction formation that achieved promising myofiber development after 14 days of culture and cell differentiation over 21 days of culture [66]. These studies highlight the current state of skeletal muscle tissue engineering using light-assisted bioprinting.

4.2 | Bone

Bone, the primary structural component of the skeletal system, contains a mineralized extracellular matrix, which imparts strength, rigidity, and elasticity characteristics [77]. Bones are classified as short (e.g., carpals), long (e.g., femur), flat (e.g., skull), sesamoid (e.g., patella), or irregular (e.g., vertebrae) [78]. Bone serves essential functions: it supports the body, protects vital organs, facilitates movement by acting as levers for muscles, [79, 80] stores key minerals such as calcium and phosphate, [81] and enables hematopoiesis through bone marrow. [81, 82] The spinal cord is a component of the central nervous system that is involved with the transmission of signals between the brain and body while being safeguarded by the spinal column, a flexible assembly of interlocking vertebrae [83].

Bone injuries and diseases are common MSK health concerns. They include fractures, which can be traumatic (e.g., spinal fractures affecting vertebrae) or pathological (e.g., caused by osteoporosis or cancer) [84]. Degenerative conditions such as osteoporosis and reduced bone density can lead to fragility fractures, while osteoarthritis and joint degeneration involve changes to the subchondral bone. [85] Bone infections, such as osteomyelitis, are typically caused by bacteria or fungi. Tumors can also affect bones, including primary bone cancers (e.g., osteosarcoma) and metastatic cancers (e.g., secondary tumors away from the primary site) [86]. Congenital disorders, such as brittle bone disease

TABLE 2 | Summary of recent musculoskeletal tissue engineering studies utilizing light-assisted bioprinting techniques.

Tissue type	Technique	Materials	Cells	Key findings	Reference
Cartilage	DLP	10% gelMA (or 10% PEGDA) dECM 0.25% LAP 0.1% tartrazine	Primary human auricular chondrocytes	Microtissue gels had higher collagen expression of collagen II and aggrecan expression than cell-laden gelMA gels	Xie et al. [43]
	DLP	15% gelMA 10% dextran 0.3% β-lactoglobulin nanoparticles 0.5% LAP	NIH/3T3 mouse fibroblasts C2C12 myoblasts SK-Hep-1 human hepatocellular carcinoma cells Rat primary chondrocytes	Higher viability and COL2A1and SOX9 expression in porous gels versus pure gelMA bulk gels	Tao et al. [50]
	DLP	5% gelMA 2% HAMA 0.1% LAP	Porcine articular chondrocytes	Ink stratification had significant zonal differences in gene expression: higher COL1A1 and ACAN and lower COL2A1, with increased gelMA concentrations	Shopperly et al. [51]
	DLP	10% DF, gelMA 10% SF, gelMA 0.25% β-TCP 0.5% R1800 0.5% LAP	Human bone marrow-derived stem cells	DF-gelMA had higher viability and Ca^{2+} deposition than SF-gelMA; β-TCP additive had a dose-dependent decrease in viability but supported calcium deposition; HAMA additive supported GAG deposition; DLP resulted in the highest ATP content across print techniques	Bedell et al. [40]
	DLP	10% gelMA 0.1% LAP 0.04% Phenol red	Human & rabbit bone marrow-derived stem cells	Cell-loaded microspheres showed higher chondrogenicity than traditional cell pellets; developed osteo-callous organoids replicating stages of endochondral ossification	Xie et al. [42]
	DLP	10% gelMA 0%–10% Silk fibroin/SG 0.3% I2959	C-28/I2 human chondrocytes	SG addition increased mechanical properties while slowing the in vivo degradation rate and maintaining good cell viability	Shen et al. [52]
	Filamented light biofabrication	0.75% HA-NB 0.84% PEG2SH 0.5% LAP	Primary infant polydactyly chondrocytes	FLIGHT gel microstructure better supported anisotropic collagen deposition, chondrogenesis, and mechanical properties versus bulk gels; potential to mimic zonal architecture and apply in situ	Puiggalí et al. [53]
	DLP	10% gelMA 1% NARMA 0.5% LAP	Rabbit articular chondrocytes	NARMA addition supports chondrogenesis in vitro and is best in vivo scaffold-to-defect integration without fibrous tissue versus gelMA alone	Huang et al. [54]

(Continues)

TABLE 2 | (Continued)

Tissue type	Technique	Materials	Cells	Key findings	Reference
	DLP	SILMA 0.2% LAP	Human septal and rabbit auricular chondrocytes Human & rabbit turbinate-derived mesenchymal stem cells	Scaffold of varying % SILMA and pattern immersed in DI water induced stable curvatures validated via FEA; chondrocytes & MSCs formed immature neo-cartilage over 8 weeks with slight stenosis in vivo	Kim et al. [55]
	DLP	4% dFuGMA 0.5% LAP	Rabbit articular chondrocytes	dFuGMA demonstrated antioxidant and antibacterial properties with a slower degradation rate and improved cartilage repair efficiency versus gelMA	Zhu et al. [31]
	DLP	10% gelMA 0.5% HAMA 0%–10% PAM 0.4% I2959/ LAP	Neonatal rat costal chondrocytes	AM addition has a positive correlation with faster cell growth; these hydrogels (10% AM) expressed an increase in COL2, AGG, and SOX-9 proteins over 14 days of culture	Jia et al. [36]
	Single-cell photolithography	PDMS mold Au mask	Rabbit articular chondrocytes	Single-step PDMS cell-imprinting achieved single-cell resolution (∼5 μm), adaptable to various photomasks and cell types	Kavand et al. [23]
	Extrusion	8% Gelatin 0.5% Alginate-tyrosine 0.05% CMC, tyrosine 0.1 mM/1 mM Ru/SPS	Human bone marrow-derived stem cells	Cell differentiation toward bone (CMC scaffold) and cartilage (ALG scaffold) over 14 days, with confirmed gene and protein expression despite culture medium components	Senturk et al. [56]
	Extrusion	3.5% Gelatin 1%–2% dECM 0.25% LAP	Goat bone marrow-derived stem cells	Bioinks supported BMSC viability and chondrogenesis (hyaline) with increased GAG and COL2 and low COL1 after 21 days	Behan et al. [57]
	Extrusion	Alginate 3% $CaCl_2$ I2959	Human umbilical mesenchymal stem cells	Double-crosslinking alginate improves its mechanical properties, stability, and printability, and can promote aggrecan, COL2, and SOX-9 gene expression	Chu et al. [28]
	Extrusion	0%–2% Hyaluronic acid 10% y-poly(glutamic) acid 0.25% LAP	Human articular chondrocytes	Higher concentrations of HA improved cell proliferation and GAG/COL2 production over 1 week, while reducing tensile strength and modulus	Lee et al. [58]

(Continues)

TABLE 2 | (Continued)

Tissue type	Technique	Materials	Cells	Key findings	Reference
	Extrusion	10% PVA-NB' dECM EDT 2 mM LAP	Teratocarcinoma-derived chondrogenic cells (ATDC5)	Higher concentrations (50%) of dECM reduced compressive strength but improved viability over 7 days, unlike PVA-NB alone	Setayeshmehr et al. [26]
	Extrusion	15% gelMA 15% Platelet-rich-plasma 0.3% I2959	Teratocarcinoma-derived chondrogenic cells (ATDC5)	PRP bioink enabled long-term growth factor release and increased cell proliferation and chondrogenic differentiation over 21 days	Irmak et al. [59]
	Extrusion	8% gelMA 8% gelMA-Tyramine 0.5 mM/5 mM Ru/SPS	Equine articular chondroprogenitor cells	Dual-functionalized ink supported neo-cartilage formation and showed superior adhesive strength, mechanical properties, and chondrogenic differentiation compared to gelMA alone	Lim et al. [38]
	FDM DLP	PCL 25% SILMA 0.3% LAP	Rabbit auricular chondrocytes	PCL/SILMA composite had similar compression strength but greater flexibility than PCL alone and supported tissue growth without in vivo stenosis	Lee et al. [30]
	Extrusion	2% NorHA 0.08% DTT 0.05% LAP	Bovine primary bone marrow-derived juvenile mesenchymal stem cells	NorHA bioink supported long-term culture over 56 days with a uniform cell distribution and increasing compressive modulus, GAG, and collagen content	Galarraga et al. [29]
	Extrusion	5% gelMA 0.25% LAP	Rat bone marrow-derived mesenchymal stem cells	Lower concentration was printable, supported cell viability, and increased chondrogenic differentiation over 21 days; *in vivo* PRP treatment promoted better regeneration versus gelMA alone	Luo et al. [60]
	Extrusion	2.5% OMA 0.05% I2959 0.2M $CaCl_2$	Human primary bone marrow-derived mesenchymal stem cells	Cryopreservation of microgels does not significantly impact cell viability or extrusion printability, showing similar DNA/ALP and DNA/GAG content from differentiation	Jeon et al. [61]
Skeletal muscle	Chaotic 2D printing	10% gelMA 0.001% Virions 0.067% LAP	C2C12 myoblasts	Low initial viability recovered by week 2 of fiber culture; Virions improved cell attachment to fibers and viability at week 4, with similar striation patterns to native tissue	Frías-Sánchez et al. [62]
	TPP	CMMC HCC Gelatin PEG Matrigel	Primary murine muscular fibroblasts Human umbilical vein endothelial cells Neural progenitor cells	Precise printed constructs directly within live mice using $\lambda > 850$ nm, leading to de novo myofiber formation over 7 days	Urciuolo et al. [63]

(Continues)

TABLE 2 | (Continued)

Tissue type	Technique	Materials	Cells	Key findings	Reference
	Extrusion	CELLINK gelMA A CELLINK GelXA FIBRIN CELLIN FIBRIN	C2C12 myoblasts	All constructs demonstrated viability, proliferation, and differentiation, but CELLINK FIBRIN displayed the best results.	Ronzoni et al. [64]
	Extrusion	10% gelMA 6%–8% Alginate 0.5% I2959 0.1 $CaCl_2$	C2C12 myoblasts	Dual crosslinked 8% Alginate-gelMA had the best cell growth, improved metabolic activity, and myotube formation over 7 days of culture	Seyedmahmoud et al. [65]
	Extrusion	2.5% ColMA 0.1% LAP	Primary murine skeletal myoblasts Neural stem cells Neural progenitor cells	Coaxial printed gel with myoblasts and neural cells led to myofiber development by 14 days of culture, with high viability and differentiation of each cell type by 21 days	Sanz et al. [66]
Ligament	DLP	10% gelMA 0.5% LAP	Human dental follicle cells	*In vivo* transplantation of bioprinted patches into mandibles produced functional periodontal ligament fibers with proper fiber orientation and stable tooth movement.	Ma et al. [67]
Tendon	Extrusion	5%–10% gelMA 0.5% LAP	Primary human tenocytes	Platelet-rich plasma-infused scaffolds improved viability and proliferation and induced angiogenic behavior; IL-1β had little impact in comparison	Del Amo et al. [25]
Bone	DLP	SILMA LAP	MC3T3-E1 pre-osteoblasts	Printed SILMA hydrogels demonstrated good cytocompatibility and supported cellular proliferation	Rajput et al. [68]
	DLP	15% gelMA 10% Dextran LAP	Rat bone marrow-derived mesenchymal stem cells	Hydrogel porosity significantly enhanced the spread, migration, and proliferation of encapsulated BMSCs	Tao et al. [69]
	DLP	40 wt% PEGDA Ru/SPS	Human mesenchymal stem cells MDA-MB-231 breast cancer cells C2C12 cells Human umbilical vein endothelial cells	Bioinks were mixed in real-time at controlled volumes (determined by infusion rates) to create both horizontal and vertical gradients with reasonably high resolution	Wang et al. [70]
	Tomographic volumetric bioprinting	gelMA LAP	Human bone marrow-derived mesenchymal stem cells Human umbilical vein endothelial cells	3D cell coculture improved early osteocyte markers (PDPN, DMP1) after 21 days, indicating accelerated osteogenic differentiation due to paracrine signaling	Gehlen et al. [71]

(Continues)

TABLE 2 | (Continued)

Tissue type	Technique	Materials	Cells	Key findings	Reference
	DLP	PEGDA LAP	NIH-3T3 fibroblast cell Human umbilical vein endothelial cells	Cell-laden hydrogels were able to replicate the mechanical moduli of native bone and vascular tissue networks	Yang et al. [72]
	DLP	ColMA LAP	Schwann cells Rat bone marrow-derived mesenchymal stem cells	ColMA bioinks supported > 95% viability with improved cell spreading and increased expression of osteogenesis-related genes compared to gelMA	Shi et al. [73]
	DLP	gelMA Alginate Hydroxyapatite LAP	Human bone marrow-derived mesenchymal stem cells	Hydroxyapatite hybrid bioinks demonstrated superior bone repair capabilities compared to pure organic bioinks	Ren et al. [44]
	DLP	Hydroxyapatite HDDA TPO	Rat bone marrow-derived mesenchymal stem cells	Hydroxyapatite scaffolds have ~ 70% porosity with various pore shapes; cubic pore-shaped scaffolds exhibited the most active cell metabolism	Liang et al. [39]
	DLP	gelMA PMMA LAP	Human bone marrow-derived mesenchymal stem cells Human umbilical vein endothelial cells	Scaffolds induced endochondral osteogenesis via iron-chelating properties, offering a novel strategy for bone regeneration	Gao et al. [74]
	DLP	MA-κ-CA bioactive silica nanoparticles LAP	MC3T3-E1 pre-osteoblast	3D MA-κ-CA/BSNP composite scaffolds exhibited good biocompatibility over 21 days of culture	Kumari et al. [75]
	Extrusion	SILMA nano-hydroxyapatite LAP	Rat bone marrow-derived mesenchymal stem cells	Addition of HAp to SILMA-based hydrogels improved osteogenic effects via M2 macrophage polarization, demonstrated through in vitro culture and validated in vivo	Zhou et al. [45]
	Extrusion	PVA dECM genipin	Teratocarcinoma-derived chondrogenic cells (ATDC5)	Introduction of SDCM into PVA-Nb lowered the compression modulus but enhanced cell viability and bioprintability	Setayeshmehr et al. [26]
	DLP Extrusion	SILMA LAP	Human lung fibroblast (MRC5) Human adipose-derived stem cells	SILMA scaffolds proved biocompatible following ISO 10993, supported osteogenic differentiation, and have preliminary results suggesting potential shape-memory properties for implant injection	Bucciareli et al. [76]

Abbreviations: CMC, carboymethyl cellulose; CMMC, 7-carboxymethoxy-4-methylcoumarin; ColMA, methacrylate collagen; dECM, decellularized extracellular matrix; DF, double functionalized; dFuGMA, degraded fucoidan glycidyl methacrylate; DTT, DL-dithiothreitol; EDT, 2,2'-(Ethylenedioxy) diethanethiol; gelMA, gelatin methacrylate; HA-NB, norbornene modified hyaluronic acid; HAMA, hyaluronic acid methacrylate; HCC, 7-Hydroxycoumarin-3-carboxylate; HDDA, 6-hexanediol diacrylate; I2959, irgacure 2959; MA-κ-CA, methacrylate-κ-carrageenan; NARMA, naringin methacryloyl; NB, norbornene; NorHA, norbornene-modified hyaluronic acid; OMA, oxidized and methacrylate alginate; PAM, polyacrylamide; PCL, polycaprolactone; PEG2SH, bifunctional thiolated polyethylene glycol; PEGDA, polyethylene glycol diacrylate; PMMA, polymethacrylic acid; PVA, poly(vinyl acid); Ru/SPS, ruthenium (Tris(2,2-bipyridyl) dichlororuthenium (II) hexahydrate)/sodium persulfate; SF, single functionalized; SG, glycidyl methacrylate silk fibroin; SILMA, silk fibroin methacrylate.

(osteogenesis imperfecta) and scoliosis, also contribute to bone-related conditions. [87]

Bone has an excellent self-regenerative capacity compared to most tissues, primarily due to the presence of osteoprogenitor cells, osteoblasts, osteocytes, and activated signaling pathways via bone morphogenetic proteins [88]. These components enable the repair of small fractures or defects through natural remodeling processes. However, larger defects, known as critical-sized defects, require external interventions such as grafts or scaffolds. Several advanced techniques are employed in bone research and repair, with tissue engineering being one of the most popular approaches, combining biomaterials, cells, and bioactive factors in order to mimic the regenerative environment of bone [89]. Use of 3D printing for bone tissue engineering is a promising strategy as it allows for the construction of patient-specific bone scaffolds for critical-sized defects via a customized CAD input [90–92]. Among various 3D printing techniques, light-assisted 3D printing has garnered significant attention from the research community.

Several studies have explored the use of photocurable materials for applications in bone tissue engineering. For example, Rajput et al. utilized DLP to create scaffolds that closely resemble the structure and mechanical properties of human tissues. Silk fibers were functionalized with glycidyl methacrylate to synthesize silk fibroin methacrylate (SILMA), a material capable of photo-crosslinking. The bioprinted SILMA hydrogels exhibited good cytocompatibility and supported cellular proliferation. [68] Bucciarelli et al. also evaluated SILMA as a suitable bioink for DLP and extrusion printing, demonstrating its biocompatibility and osteoconductivity. In addition, they evaluated the shape-memory properties of a scaffold made from this material [76]. Tao et al. used DLP-based bioprinting for processing of bone marrow stem cells (BMSCs) mixed with a gelMA/dextran emulsion. The 3D-bioprinted hydrogel supported the proliferation and migration of the encapsulated BMSCs. The material also triggered activation of the YAP signaling pathway, which promoted the osteogenic differentiation of BMSCs [69]. Gao et al. investigated gelMA and polymethacrylic acid (PMAA) hydrogels and found that the addition of PMAA improved the ink viscoelasticity and iron-chelating properties of these biological scaffolds, which in turn promoted endochondral osteogenesis. This approach offered a promising strategy for advancing bone regeneration [74]. Yang et al. utilized multimaterial DLP bioprinting to reproduce the complex mechanical and structural features of natural tissues in vitro, as shown in Figure 4A. A PEGDA-AAm bio-ink was formulated and 3D-printed to prepare multicomponent, cell-laden hydrogel constructs with various modulus levels. The results indicated that by incorporating cell-laden hydrogels, the approach successfully mimicked the mechanical properties of biological tissues (e.g., bone and vasculature) [72].

Calcium phosphate materials, such as hydroxyapatite (HAp), are an inorganic constituent of bone. Ren et al. developed bioinks based on gelMA and alginate with HAp to fabricate scaffolds via DLP techniques. The gelMA/alginate/HAp tissue scaffold

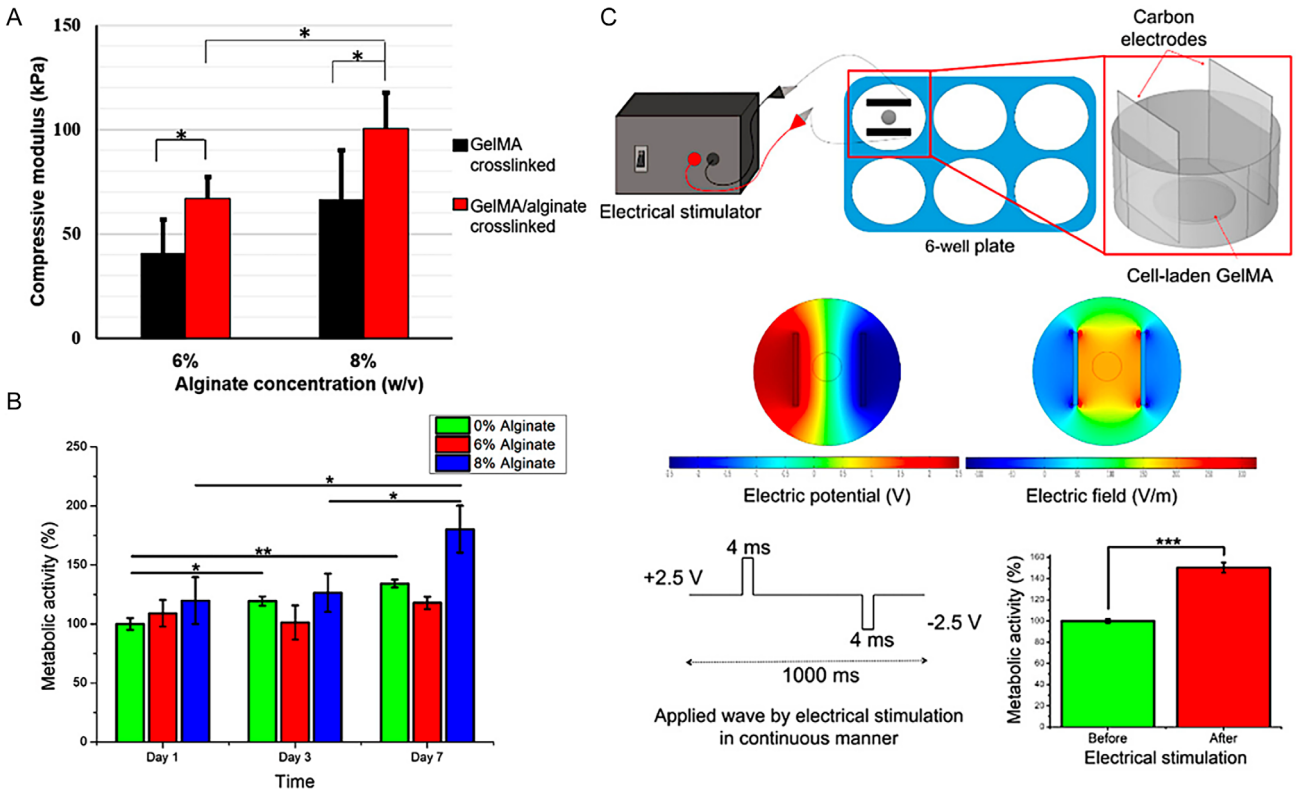

FIGURE 4 | Seyedmahmoud et al. varied scaffold properties through bioink formulation and culture conditions for skeletal muscle tissue engineering. (A) Compressive modulus of gelMA hydrogels with varying alginate concentration, (B) Cell metabolic activity over 1 week from the same hydrogels, (C) Electrical stimulation set-up for cell-laden hydrogels and metabolic changes due to applied electrical pulses. Reproduced under terms of the CC-BY license [65]. 2019 by the Authors, published by MDPI.

demonstrated notable bone repair functionality in vivo compared to pure organic bioinks. [44] Liang et al. also formulated a DLP bioink with HAp manufacturing scaffolds using various pore shapes with an approximate 70% porosity. Their results suggested that cubic pore-shaped scaffolds exhibited the most active cell metabolism [39]. Various other inorganic biomaterials have also been utilized in DLP printing for bone tissue engineering. Kumari et al. applied DLP printing using methacrylate-κ-carrageenan (MA-κ-CA) and bioactive silica nanoparticles (BSNPs). Their results showed that the 3D-printed composite scaffolds of MA-κ-CA and BSNPs demonstrated biocompatibility for bone tissue engineering via in vitro and in vivo experiments over 21 days [75]. Commercial photoresin and HAp have also been used in the DLP approach. Ge et al. used $MgO/Ca_3(PO_4)_2$ photosensitive resin with a dispersant, demonstrating that a high magnesium oxide content improved the mechanical properties, similar to that of cancellous bone, while exhibiting good biocompatibility [93]. Zhang et al. studied the degradation properties of a photosensitive resin with HAp and various amounts of calcium silicate. Their results showed that the scaffolds demonstrated good cytocompatibility, promoting cell proliferation and differentiation, and increased levels of calcium silicate were able to maintain scaffold compressibility after immersion tests up to 14 days [94].

Tomographic volumetric bioprinting has recently emerged in popularity for the rapid solidification of cell-laden hydrogel constructs. Gehlen et al. utilized volumetric bioprinting with a gelMA-based bioresin to facilitate a 3D endothelial coculture in order to create heterocellular bone-like constructs. The results of the study showed that the human mesenchymal stem cells (MSCs) and human umbilical vein endothelial cells in the 3D cocultures displayed elevated expression of early osteocyte markers after 21 days, indicating accelerated osteogenic differentiation [24]. Extrusion with photocurable ink is another approach for developing bone tissue scaffolds. Zhou et al. applied an extrusion technique using methacrylated silk fibroin and nano-HAp hydrogel with LAP. The results showed that the addition of HAp provided a composite hydrogel bioink for bone regeneration and evaluated its performance via the ALP assay and transcriptomic analysis [45]. As shown in Figure 4B, Shi et al. synthesized methacrylated collagen (ColMA) bioinks, which demonstrated similar printability to gelMA in both DLP and extrusion-based bioprinting, while exhibiting superior formability. BMSC-laden ColMA bioinks showed > 95% viability, improved cell spreading, and a higher level of expression of osteogenesis-related genes compared to gelMA [73]. These studies significantly advance the field through the evaluation of the feasibility of multimaterial photoresin-based bioprinting to prepare complex, functionally relevant structures for TERM applications. Bone scaffolds are among the most clinically advanced tissue-engineered constructs, largely because bone has a strong intrinsic capacity for self-regeneration, which has supported the widespread use of acellular, osteoconductive scaffolds. In contrast, cell-laden bone scaffolds aim to further enhance regeneration by delivering osteogenic or progenitor cells, particularly for large or compromised defects, although their clinical translation remains limited by manufacturing, cost, and regulatory challenges. Overall, these approaches are complementary, with acellular scaffolds suited for routine clinical use and cell-laden systems offering potential benefits in more complex cases.

4.3 | Cartilage

There are three types of cartilage: elastic, articular, and fibrocartilage. For MSK purposes, this section primarily focuses on articular cartilage (AC), the most abundant type. AC is predominantly located in joints such as knees, elbows, hips, and shoulders. AC, also known as hyaline cartilage, lines the subchondral bone within the joint cavity to reduce friction and provide cushioning for wear resistance [2, 95]. Cells within this tissue are known as chondrocytes, which make up only 1-5% of mature AC tissue. Extracellular matrix (ECM) components secreted by the small cell population constitute the remaining 95%-99% of adult cartilage. The ECM of cartilage includes varying concentrations of proteoglycans, water, elastin, collagen, noncollagenous proteins, glycoproteins, and inorganic ions, depending on zonal structure. [95].

Cartilage consists of three zones: a superficial layer, a medial layer, and a deep layer. Each layer has distinct characteristics and contributes to the overall function and performance of AC. The superficial zone, closest to the articular space, is responsible for lubrication via small, elongated chondrocytes that produce type I collagen, hyaluronate, and phospholipids. The medial layer accounts for 40-60% of the AC volume and houses large, round chondrocytes that secrete type II collagen to resist shear forces. The deep layer is the largest zone, where chondrocytes are organized in column-like structures to help resist tensile and compressive forces [95]. An additional zone that is important to the joint cavity is the calcified zone. This region represents the interface between mineralized and unmineralized tissue, which stabilizes the deep-layer collagen within subchondral bone [95].

Several studies have evaluated photocurable materials for use in cartilage tissue engineering. Among these, gelMA is the most common precursor, often referred to as a “universal ink”; it has been used across numerous tissue types and fabrication techniques, as discussed throughout this review. GelMA is the product of solubilized gelatin and methacrylic anhydride (MA). Functionalization often preludes crosslinking as the chemical bonds formed by added functional groups are stronger than physical crosslinks, which are often temperature-dependent and reversible. The level of functionalization is variable, as explored by Bedell et al. Compared to a less functionalized material, dual-functionalized gelMA exhibited higher cell viability and increased calcium deposition after 14 days of culture. Although these results suggest that a higher polymer network density may be beneficial, it is important to note that the single-functionalized gelMA was porcine-derived, whereas the dual-functionalized material was derived from human skeletal tissue. This difference in material origin may have also played a role in the behavior of seeded human BMSCs. [40] Lim et al. further investigated dual functionalization by incorporating both MA and tyramine to produce gelMA-Tyr scaffolds. Their findings demonstrated a 15-fold increase in adhesive strength to cartilage tissue, enabling the gel to act as a bioglue for delivering articular chondroprogenitor cells to defect sites. [38] Beyond gelatin-based systems, MA is a widely used functional group for other hydrogel systems. Alginate is a popular hydrogel due to its inherent biocompatibility; however, its lack of mechanical strength has prompted researchers to explore dual-crosslinking strategies [28, 56, 61]. Chu et al. investigated dual functionalization of alginate using sulfhydryl groups and conjugated double bonds

to allow the formation of ionic and covalent bonds. This double-crosslinked system exhibited increased strength and stability without compromising cell viability or chondrogenic differentiation [28]. Despite the added fabrication complexity, dual functionalization and double crosslinking provide an effective strategy to improve the performance of single polymer hydrogels. An alternative approach to dual crosslinking is changing the precursor material itself. Zhu et al. developed degraded fucoidan-glycidyl methacrylate hydrogels that exhibited superior mechanical properties and swelling capacity compared to gelMA. This bioink also outperformed gelMA in cartilage repair, promoting increased chondrogenic gene expression (e.g., SOX9, ACAN, and COL2:COL1) and exhibiting antioxidant and antibacterial properties [31].

Many researchers have utilized multimaterial systems to improve scaffold performance [30, 39, 41, 31, 40, 42]. Modifications to gelMA, including the incorporation of methacrylate-modified naringin, hyaluronic methacrylate, dextran, and silk fibroin, have been used to enhance scaffolds beyond gelMA-only hydrogels [50–52, 54]. Bedell et al. demonstrated how copolymer choice significantly influences BMSC differentiation in gelMA-based hydrogels. Regardless of culture medium (e.g., osteogenic or chondrogenic medium), the addition of HAMA led to increased GAG deposition, whereas β-TCP promoted calcium deposition over time. Moreover, while HAMA had no effect on viability, β-TCP had a negative dose-dependent impact on human BMSCs. These findings indicate the potential of such material combinations in osteochondral tissue engineering, particularly when using DLP techniques, which demonstrated higher cell viability than inkjet- and extrusion-based printing methods [40]. Shopperly et al. demonstrated that varying the HAMA-to-gelMA ratio altered ECM composition, offering a useful approach to replicate the zonal characteristics of native cartilage tissue. Bioinks with low HAMA (0.4%) and high gelMA (4%) concentrations resulted in lower cell densities, but higher GAG and collagen II production compared to formulations with more balanced or reversed ratios (2.5% gelMA:1% HAMA and 1% gelMA:1.6% HAMA). These differences were clearly illustrated in a stratified model, in which all three bioinks were layered with visually distinct levels of collagen II and GAG deposition after 14 days of culture [51]. Xie et al. combined cartilage-derived decellularized extracellular matrix (dECM) and chondrocyte aggregates with a gelMA hydrogel to produce 3D auricular scaffolds. Compared to the structures containing gelMA alone, cell-laden gelMA, and cell-laden gelMA-dECM ink, the composite gelMA-dECM scaffolds demonstrated the greatest degree of neocartilage formation, including increased cell proliferation and expression of COL2A1 and ACAN [43]. Silk fibroin has also been used as a copolymer to slow gelMA scaffold degradation in vivo and in vitro, resulting in higher compressive strength and prolonged ECM production compared to gelMA alone. However, this improvement was not sustained over extended culture periods (3 weeks versus 2 weeks), as matrix production did not sufficiently compensate for increased scaffold degradation, thereby compromising long-term structural integrity and mechanical strength [52].

Synthetic and hybrid material systems have been increasingly explored as copolymers in cartilage scaffolds to address the persistent trade-off between biocompatibility and mechanical performance [30, 36] Rather than relying solely on natural hydrogels, several studies have demonstrated that controlled incorporation of synthetic components enables tunable stiffness, degradation, and structural stability while preserving chondrogenic potential. For example, Jia et al. increased the acrylamide concentration to enhance the compression capacity and slow the degradation of gelMA/HAMA hydrogels without compromising short-term cell viability over 7 days or chondrogenic protein expression over 2 weeks of in vitro culture [36]. Similarly, Lee et al. employed FDM and DLP techniques to fabricate PCL-Sil composites that displayed greater flexibility than PCL alone while maintaining comparable axial compressive strength. Using dual printing methods, they produced scaffolds for tracheal cartilage development that supported in vivo tissue regeneration without inflammation or lumen narrowing [30]. These rigid-soft hybrid systems highlight a straightforward but effective method for mechanical reinforcement.

Beyond polymer concentrations and composite composition, scaffold porosity has emerged as a significant design parameter governing nutrient transport, cell morphology, and matrix deposition. Comparative studies show that porous hydrogel constructs outperform bulk hydrogels in supporting cartilage formation. For instance, emulsified gelMA scaffolds containing dextran microdroplets stabilized via β-lactoglobulin nanoparticles promoted cell spreading, higher viability, and increased cartilage matrix deposition compared to bulk gelMA following implantation in rats [50]. Similar porosity effects have been observed in gelMA-based, SILMA-based, and SG-gelMA hybrid scaffolds [50, 52]. In contrast, dense, bulk hydrogels with limited surface area and diffusion capacity fail to sustain long-term cell proliferation, with Shen et al. reporting growth arrest beyond 5 days of culture [52]. Collectively, these findings suggest that porosity is not merely an optimization parameter but a prerequisite for scaffold maturation.

From a fabrication standpoint, the majority of studies discussed above investigated cartilage scaffold fabrication via DLP printing techniques using either commercial or custom systems. The combination of photocuring with extrusion printing or molding has used material systems similar to those described in the aforementioned studies [26, 29, 38, 57–60]. A notable extension among light-based 3D strategies is FLight biofabrication, a custom high-throughput technique that has been used to generate macroporous hyaluronic acid-based hydrogels with a specific focus on aligned microfilament formation. The alternating microchannels and microfilaments provided an excellent construct design for replicating cellular stacking and anisotropy of the cartilage deep zone. Compared with bulk hydrogels, Flight resulted in superior cartilage tissue maturation, with a distinct uniaxial organization of cells and collagen (Figure 5). Puiggalí et al. further demonstrated that this approach is capable of producing up to 10 samples every 3.3 s. Proof-of-concept studies also showed the feasibility of fabricating multilayered constructs with distinct zonal organization, showcasing the potential of this technique for in situ cartilage defect repair [53]. Taken altogether, these studies indicate a clear shift away from single-material, bulk hydrogels toward multicomponent and architecturally complex scaffolds. This convergence of material chemistry, scaffold design, and advanced light-based fabrication represents a crucial step toward our understanding of light-based 3D printing technologies and

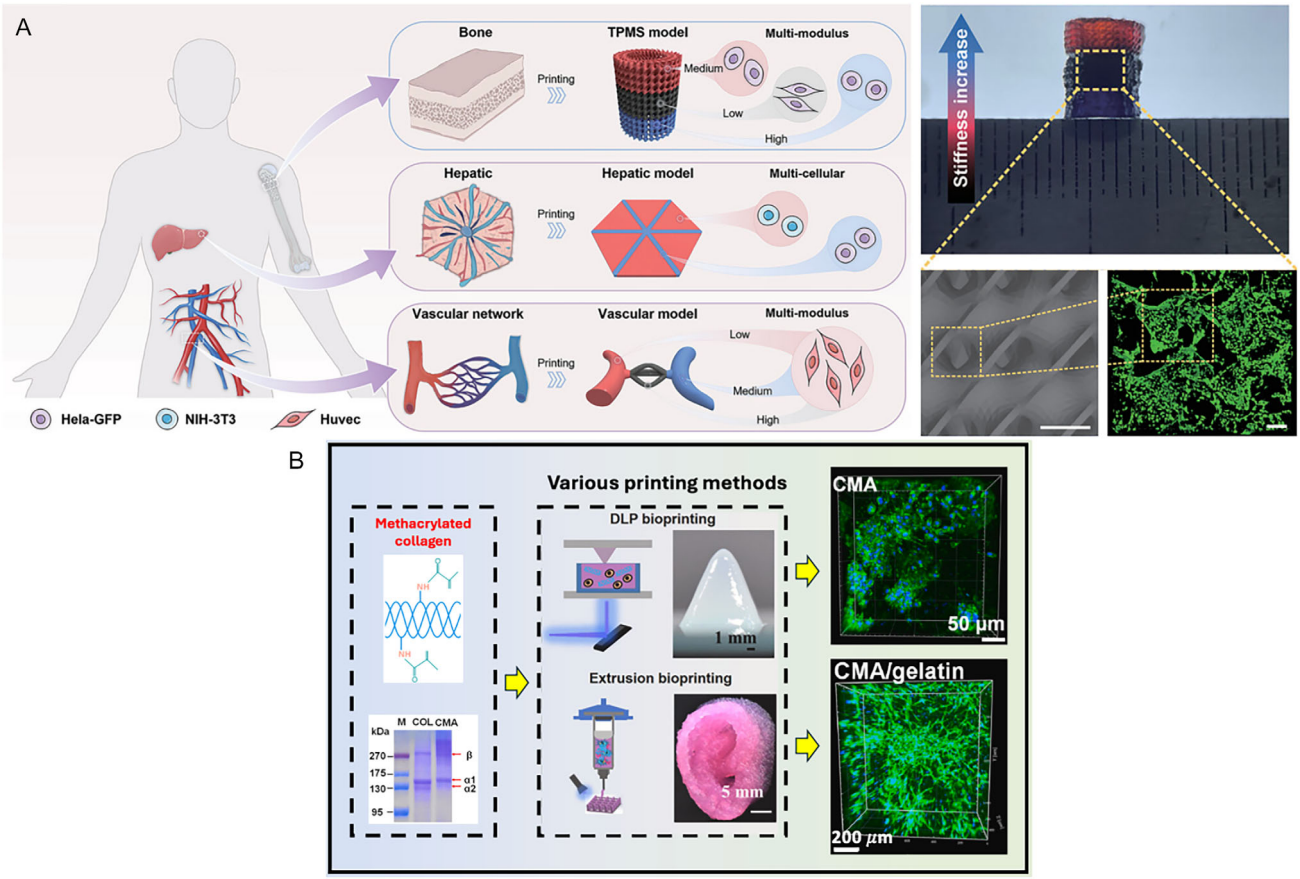

FIGURE 5 | Utilization of light-based bioprinting for bone tissue engineering. (A) Schematic representation of hydrogel constructs used as in vitro models to mimic heterogeneous human tissue structures. Reproduced with permission [72]. 2024, Wiley. (B) Multimaterial DLP bioprinting of heterogeneous hydrogel constructs to mimic bone tissue with varying moduli. Reproduced with permission [73]. 2023, Elsevier.

their compatible biomaterials for engineering cartilage constructs that more closely replicate native tissue (Figure 6).

4.4 | Tendons and Ligaments

Tendons and ligaments are connective tissues that support body stability and movement. Ligaments are comprised of mostly collagen fibers in addition to a lower amount of glycoproteins and elastin. This tissue type is responsible for joint stabilization via bone-to-bone connections. Ligament tissue is two-thirds water, which assists in handling cyclic load-bearing activity that occurs in these regions. Similarly, tendons mainly consist of collagen in large anisotropic bundles that are arranged in fascicles. Tendons are responsible for posture and movement by transferring muscular forces to bone. Tenoblasts and tenocyte fibroblasts are responsible for producing collagen and other proteins, such as elastin, which enable flexible motion during tissue stretching and compression. Throughout the body, tendons vary in size and shape, yet overall, this tissue is very stiff with high tensile strength [2, 5] Common injuries with these tissues include tendinopathy and tissue rupture. Tendinopathy involves generalized pain and inflammation; these processes are typically associated with progressive tissue degeneration over time [25]. Ruptures can occur in both tissue types, leading to instability, pain, and even disability in some cases. While small tears heal over time, the regenerated tissue typically performs with lower functionality due to a loss of stiffness. The gold standard for larger ruptures includes autografts, allografts, or synthetic suture materials [5]. Tissue engineering via 3D bioprinting can expand our understanding of tendon and ligament pathologies through in vitro models and alternative treatment solutions.

Two studies were found that suited the inclusion criteria for this review. Ma et al. investigated cell-laden gelMA scaffolds for implantation as periodontal ligament patches. DLP printing was used to create an array of hydrogel pillars embedded with human dental follicle cells that were capable of osteogenesis, neurogenesis, and angiogenesis. The constructs were implanted within dogs and monitored for 12 weeks, demonstrating properly oriented fiber growth, clinical biocompatibility, and promising regeneration of the periodontium[67] Del Amo et al. investigated bioprinted tendon grafts functionalized with inflamed and non-inflamed host tissue. They discovered grafts infused with platelet-rich plasma activated inflammatory pathways and induced several downstream mechanisms involved with angiogenesis, along with increased cell viability and proliferation. They hypothesized that scaffolds of this nature can play a role in reparative inflammation as a necessary step in healing; however, detailed knowledge of these mechanisms is currently unavailable [25]. There is a lack of research using these techniques to investigate tendon and ligament tissue engineering, which hopefully can be remedied in

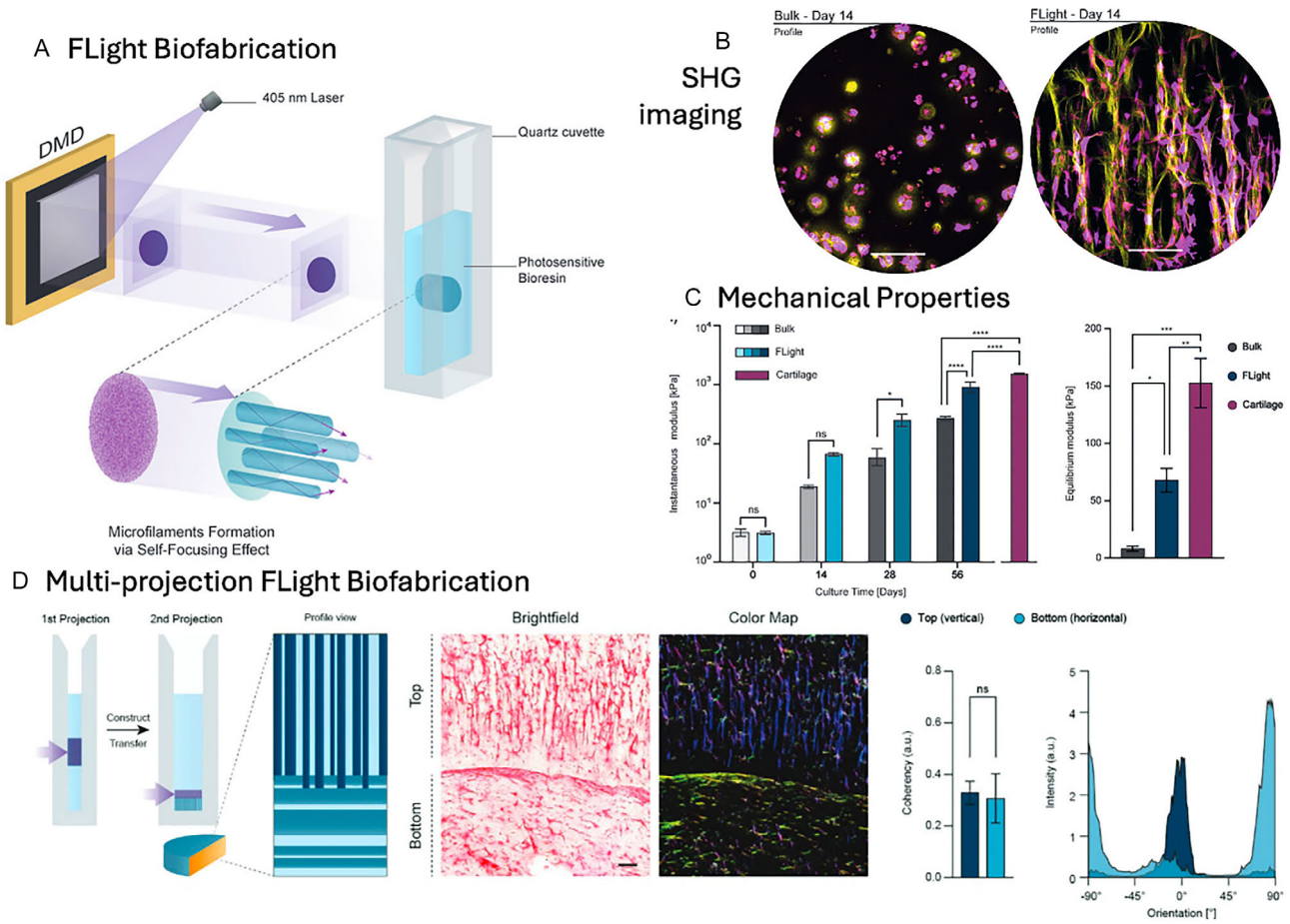

FIGURE 6 | Puiggalí et al. utilized a novel light-based bioprinting technique for cartilage tissue engineering. (A) Schematic of filamented light (FLight) biofabrication. Light projection from a digital micromirror device (DMD). Optical noise creates a speckle pattern that results in crosslinked microfilaments and microchannels. (B) Second harmonic generation (SHG) imaging of bulk and FLight hydrogel profiles after 2 weeks, highlighting cell morphology (magenta) and collagen distribution (yellow), bar: 100 μm. (C) Mechanical properties of bulk and FLight samples over time. (D) Multiprojection FLight schematic to develop vertical + horizontal collagen orientation. Images show collagen staining (red). Plot quantifies collagen fibril alignment. Reproduced under terms of the CC-BY license [53]. 2023 by the Authors, published by Wiley.

future work. This is possibly due to a limitation of the review itself, namely the use of a single set of search terms across two databases. However, the authors believe the low number of studies could be due to both technical difficulties and a lack of clinical need compared with other tissue types. These tissues have highly complex mechanical properties due to their material composition and geometric alignment, which are very difficult to emulate synthetically. Unlike bone tissue, where ceramic powder and synthetic polymers can be incorporated to improve strength, tendons and ligaments also must retain elasticity. Furthermore, bone has a high turnover rate and high vascularization, leading to better regenerative capabilities. Neither of these is true for connective tissues. While there is a clinical need for tendon and ligament studies, this need is different and affects a smaller population. For highly prevalent bone disorders such as osteoporosis and fractures, developing bone-on-a-chip or other in vitro models to evaluate pathology and therapeutics is an important area of research. The most common injury to tendons and ligaments is a partial or complete rupture. While an on-chip model can evaluate therapeutic products to instigate self-healing, in most cases, a surgical repair is required. Changing current therapies for connective tissue treatment faces greater technical and clinical adaptation challenges.

5 | Discussion and Future Perspectives

Light-assisted 3D bioprinting offers control over scaffold architecture and composition for tissue engineering applications. Unlike traditional cell seeding methods, 3D bioprinting can integrate cells within more complex designs, including multicellular and multimaterial structures. This capability enhances the potential to produce more sophisticated tissue models [4]. While the technologies offer promise, several challenges remain, such as improving the efficiency, scalability, and compatibility of the materials and processes used in light-assisted 3D bioprinting. Focused efforts are needed to overcome these obstacles and realize the full capabilities of light-assisted 3D bioprinting for TERM applications.

5.1 | Understanding the Long-Term Impact of Light-Assisted 3D Printing Mechanisms on Cell Growth and Development

One important issue in light-assisted bioprinting is understanding how the printing process and photocrosslinking mechanisms affect cell behavior. Several factors, including mechanical forces,

print speed, and total print time, affect the printing process; the use of photocuring adds additional factors such as total light absorption and chemical by-products generated during light-activated crosslinking reactions [35]. The potential cytotoxic and mutagenic effects associated with these mechanisms are not yet fully understood. Using higher light intensity or longer light exposure can improve printing resolution; however, these parameters have also been shown to affect cell viability and growth adversely [38, 96]. Moreover, Lim et al. demonstrated how in situ UV irradiation can be harmful to embedded cells as well as surrounding healthy tissue. Investigating gelation chemistries that consume harmful radicals or developing target-specific photoabsorbers for bioink could improve cell protection [38]. If the affected pathways or specific cytotoxic by-product components were better understood, appropriate cell protection mechanisms could be incorporated into light-assisted bioprinting techniques, thereby supporting the wider adoption of this approach in TERM.

Similar to other crosslinking mechanisms, photocrosslinking methods must be optimized on a case-by-case basis. Other studies have highlighted how high crosslinking densities, while beneficial for enhancing stability, degradation, and mechanical properties of a scaffold, may adversely affect cell proliferation and differentiation [53, 65]. Zhang et al. reported how introducing a second crosslinking mechanism into their MSC-laden hydrogels inhibited the development of uniform cell distribution and differentiation [97]. While these challenges persist in photocrosslinking techniques, they are not insurmountable. The existing variety of initiators and absorbers remains largely unexplored; 66.7% of studies included in this review used LAP as their reactive group, and only three utilized an absorber (Figure 7). Evaluating novel biomaterials compatible with light-assisted printing is an important consideration; understanding the advantages and disadvantages of existing components can better inform this process. For example, although LAP is the most commonly used photoinitiator in these studies, Ru/SPS has been shown to achieve more efficient crosslinking and lower cytotoxicity in certain hydrogels [98, 99].

To understand the advantages and disadvantages of printed scaffolds and the influence of printing mechanisms, the use of longer-term cultures should be considered. Most studies considered a shorter-term culture period ranging from 14 to 28 days [28, 36, 51, 56, 57, 62, 64]. Galarraga et al. demonstrated that after culturing for 56 days, cell viability in norbornene-modified HA hydrogels remained high, while ECM formation led to an increase in the compressive modulus from 5.2 kPa to 42.0 kPa. This study highlights the potential for significant tissue maturation over extended culture periods [29]. Understanding how light-assisted bioprinting influences cell growth and differentiation over long-term periods is an important consideration for advancing the 3D bioprinting field.

While assessment of gene expression, viability, and mechanical properties is important, a limited number of studies in this review performed advanced functional assessment on their mature tissue scaffolds. This represents a clear gap, since marker expression does not equate to functional maturation. However, this raises a new question. What is a standard, measurable output of functional maturity for each tissue type? Several studies have attempted to answer this question. Capel et al. and Mestre et al. fabricated muscle models using physical and chemical crosslinking methods; they measured twitch and tetanic contractile forces via electrical field stimulation [100, 101]. To achieve the near-frictionless behavior of native cartilage, studies have turned to physical and chemical surface modifications of hydrogels. Native cartilage coefficient of friction ranges between 0.001 and 0.03 MPa; Xi et al. utilized photolithography to mold cartilage scaffolds and achieved coefficient of friction values 20–30 times over this range [102]. Future studies should incorporate performance-based metrics that better predict in vivo function, such as the contractile force of bioprinted muscle, the tribological properties of bioprinted cartilage, and the fatigue loading of bioprinted connective tissue; these properties should ideally be measured after extended maturation periods and correlated with relevant in vivo benchmarks.

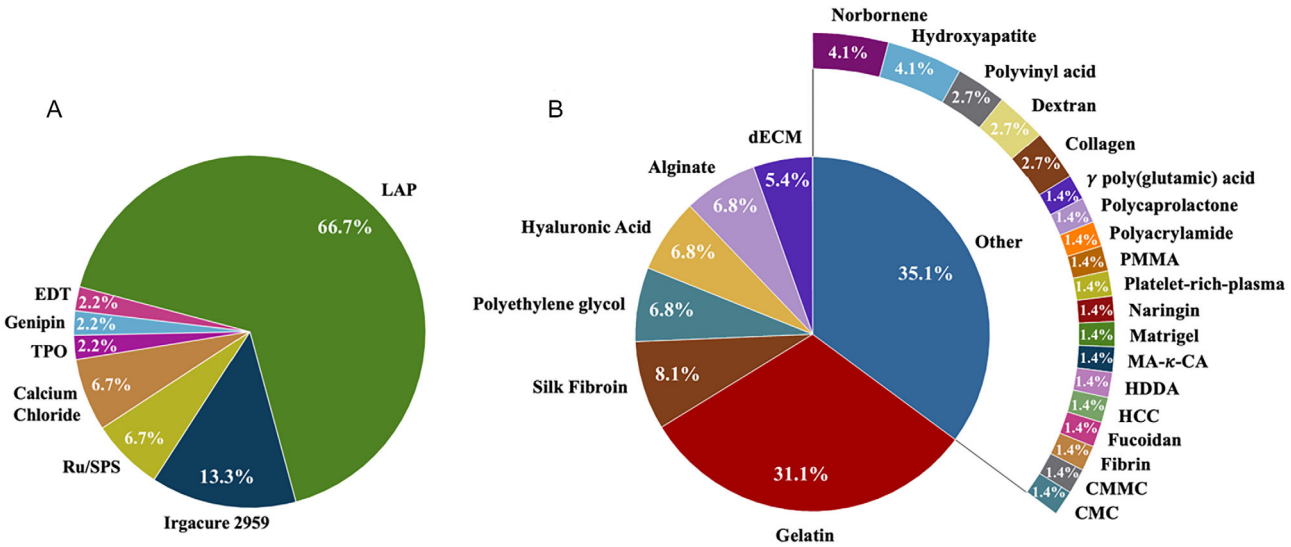

FIGURE 7 | Distribution data of photoreactive materials generated from articles included in this review. (A) Summary of photoinitiators utilized within studies for light-assisted bioprinting of musculoskeletal tissue engineering. (B) Summary of polymer materials utilized in studies for light-assisted bioprinting of musculoskeletal tissue engineering.

5.2 | Addressing Insufficient Mechanical Properties of Engineered 3D Tissues

A common concern among hydrogel scaffolds is their lack of appropriate mechanical strength. Many researchers have attempted to resolve this issue by modifying common materials such as gelMA via increasing crosslinking density or forming secondary polymer networks. Despite these additions, few scaffolds have achieved results matching those of native tissue. This is especially important for musculoskeletal tissues whose function critically relies on managing applied loads in an asymmetric and cyclic manner. Cartilage tissue, for example, undergoes heavy cyclic compression during movement and typically has an elastic modulus between 0.1 MPa and 6.4 MPa [53]. Most studies have achieved moduli in the kPa range in acellular scaffolds [43, 51, 52, 54, 56]. One study utilizing Flight-fabricated scaffolds achieved an instantaneous modulus of ~1 MPa after 56 days of culture, a tenfold increase over its performance on day 14; however, the equilibrium modulus for these samples was approximately two times lower than that of native cartilage [53]. While the instantaneous response is important for load bearing, the repetitive load application requires quick recovery after deformation. A key element in the success of this technique was achieving cellular alignment through uniaxial microsized channels. Anisotropic mechanical properties are well-established in musculoskeletal tissues. Directional materials and cellular alignment can be induced through several methods: topographical or internal cues such as channels, grooves, and filaments; process-driven methods like shear-induced alignment during extrusion; and external stimulation systems. Integrating external electrical, ultrasound, or mechanical cues has been shown to enhance the overall performance of constructs by directing cell orientation and matrix deposition [65, 101, 103]. Since hydrogel design requirements are tissue-specific—for example, skeletal muscle has a much lower modulus than cartilage [63, 65, 104],—material selection must match native mechanics. To address these differences, multimaterial approaches (e.g., natural hybrid hydrogels, natural-synthetic composites) can be utilized to enhance printability and introduce controlled heterogeneous scaffold properties [17, 72]. Gradient scaffolds have gained traction in engineering tissue interfaces due to their gradient biochemical and biophysical cues. Gradients in stiffness, signaling molecules, and porosity can steer cell migration, differentiation, and organization [92, 105]. These scaffolds offer practical ways to reproduce tissue heterogeneity and guide cell alignment to improve functional outcomes. Addressing these design challenges will improve the reproducibility and performance of mechanics-dependent tissue scaffolds.

In addition to crosslinking, alignment, and gradient modifications, studies have shown that the initial stiffness of a hydrogel plays a significant role in determining its performance. Cartilage tissue was found to mature better with higher matrix deposition and mechanical properties in gels with an initial stiffness of ~1 kPa when compared to gels with an initial stiffness of ~10 kPa [106]. While most bone tissue scaffolds have a substrate stiffness > 30 kPa, it should be noted that softer scaffolds may provide a greater benefit in long-term culture [107, 108]. The mechanical performance of an ink must be balanced with its printability, which in many cases is dependent on ink rheology. In extrusion printing, shear-thinning inks are essential for cell survival under high shear stress. In light-based printing, low-viscosity inks are important to achieve an appropriate cure depth. Higher precursor concentrations can increase the compressive strength and viscosity of an ink; however, these changes often conflict with efforts to optimize ink homogeneity and cell viability. Chu et al. modified the hydrophilicity of alginate chains to mitigate this effect and produced a double-crosslinked gel with a lower viscosity than a single-crosslinked gel; this approach obtained printability and a mechanically stronger ink [28].

This review highlights an overall lack of variety in available biomaterials. However, despite similar materials, cross-study comparisons are difficult due to differences in fabrication processes. Using a widely adopted biomaterial like gelMA as a control material can help establish a baseline across bioprinting techniques, including light-based and other methods. Since fabrication process and construct geometry significantly influence the mechanical properties of printed tissues, this would be an important step towards understanding the limitations and benefits of chosen biomaterials.

5.3 | Exploring the Scalability of Tissue Scaffolds for Mimicking Complex Human Tissue

The scalability of 3D-printed tissue scaffolds presents several opportunities for future work. Developing novel bioinks and printing methods is a time- and resource-consuming process. To improve efficiency, predictive models, such as the Bayesian optimization algorithm proposed by Chen et al., enable the prediction of critical properties, such as the compression modulus of printed scaffolds, based on polymer concentration, photoinitiator concentration, light intensity, and exposure duration [27]. This approach could help streamline the design of custom scaffolds with optimized properties. Advancements in volumetric printing can also aid this process due to rapid fabrication using smaller material volumes compared to layer-by-layer approaches seen in DLP and SLA. VAM could also address a second challenge: print construct size. Current printed tissues are limited to small animal models, which are associated with less physiological relevance (Figure S1). While optical attenuation can limit the maximum achievable cross-sectional size, recent hardware innovations such as helical projection and roll-to-roll tomographic printing have partially mitigated these constraints. Continuous VAM demonstrated printed constructs with approximate 30 mm cross-sectional dimensions at a fabrication rate of 1.75 $mm^3\ s^{-1}$, and tomographic VAM has achieved construct sizes exceeding 60 cm in length with ~200 μm resolution using roll-to-roll systems [109, 110]. Although systematic comparative scalability studies remain limited, these examples support VAM as a promising route toward scalable constructs beyond the limitations of print platform size and tissue construction resources that currently restrict the use of 3D printing for large animal- and human-sized applications. Further still, large-scale tissue constructs require vascularization to support sufficient nutrient and waste exchange for maintaining cell viability. Research into mimicking vascular networks to allow for more physiologically-relevant scaffold sizes and organ-like constructs is underway, but not yet fully incorporated into the field [4, 111].

Advances in bioinks also bring challenges related to variability and reproducibility. Lab-to-lab and batch-to-batch variations in ink composition can lead to inconsistencies in printed structures, affecting their mechanical and biological properties. As bioprinting transitions to clinical applications, the complexity of ink preparation becomes a key barrier to future standardization and large-scale manufacturing. As previously discussed, an assortment of commercially available inks exists, but the number of materials in this format is limited. This parameter underscores the need for continued innovation in bioprinting technology, particularly in developing vascular networks that can support larger tissue scaffolds and in standardizing photocurable ink production.

5.4 | Organ-on-Chip Application

Light-based bioprinting technologies have emerged as powerful tools for engineering complex musculoskeletal tissues within organ-on-chip (OOC) systems, in which high spatial resolution, material versatility, and microscale biomimicry are critical parameters. DLP and SLA are used due to their capability to fabricate microscale features (15–100 μm resolution) at high speed using photopolymerizable bioinks [112]. These hydrogels can be patterned into aligned or porous architectures that promote myoblast alignment or osteogenic differentiation [113]. GelMA-based constructs printed via DLP have been used to create myofiber-aligned structures suitable for muscle-on-chip systems [114]. For applications that require ultrafine features, such as recapitulating the nanoscale topography of bone lacunae or guiding neuromuscular junction formation, TPP offers sub-micrometer resolution [115, 116]. In comparison to traditional light-based bioprinting methods such as DLP and SLA, VAM enables faster fabrication of complex structures in a single step with dynamic light projection technology. Bernal et al. employed VAM to generate gelMA-based vascular scaffolds for use as vascularized bone-on-chip or muscle-bone interface chips for modeling tissue crosstalk [117].

Light-assisted extrusion-based bioprinting combines the structural fidelity of extrusion with light curing, allowing fabrication of mechanically graded or particle-laden bioinks. This approach is beneficial for printing muscle-bone interface models within OOC platforms. GelMA-hydroxyapatite or methacrylated collagen-bioactive glass can be printed into chips to support both soft and mineralized tissue formation [118, 119]. Allen et al. showed that extrusion-based photocuring of gelMA-HAp constructs enhanced mechanical integrity and osteogenic outcomes, which is beneficial for load-bearing bone-on-chip devices [118]. To replicate interface regions such as tendon-bone, studies have utilized DLP to print biphasic scaffolds with distinct mechanical and cellular microenvironments that exhibit potential for interface-on-chip systems [76, 120]. In brief, light-assisted methods are well suited for OOC fabrication due to their high resolution, imaging transparency, and capability for the integration of microchannels. As the field evolves, incorporating photoresponsive hydrogels, visualizable constructs, and multimaterial printing strategies will be essential for developing physiologically relevant, high-throughput OOC platforms to study musculoskeletal development, regeneration, and disease modeling.

5.5 | Commercialization and Translation of 3D Tissue Scaffolds for Clinical Use

Despite significant advancements in 3D bioprinting technologies, there are currently no clinical studies directly involving the bioprinting of human MSK tissues. In terms of translational medicine, one key question remains: are current 3D-printed scaffolds of sufficient size and stability for therapeutic use? While promising in in vivo animal studies, the time-consuming nature of high-resolution light-based 3D bioprinting poses a significant challenge for clinical and industrial-scale applications. Current research focus has shifted to extrusion-based systems with photocrosslinking mechanisms for stabilization. A handheld extrusion device called the Biopen, developed by AdBioink, was designed to support in situ regenerative medicine. These commercial printers utilize a combination of extrusion-based bioprinting with a visible light unit for photocuring, allowing direct application of hydrogels on damaged tissue, including those with curved surfaces. As with typical extrusion printing, the speed, ink composition, photoinitiator concentration, and light source in the portable system can all be modified to optimize the printing process as desired [121]. Other noncommercial devices focus on investigating in situ bioprinting options as well [29, 38, 63]. One such study envisions a carrier system where an ACPC-laden gelMA-Tyr bioink can be directly extruded into chondral defects and crosslinked via a photocuring unit. This approach also targeted the integration of printed materials with surrounding tissue to promote healing and regeneration [38]. Yet another approach utilized infrared TPP printing to crosslink injected bioinks within live mice, successfully integrating with skin, skeletal muscle, and brain tissues. The authors were able to direct cellular orientation and scaffold positioning at these anatomical sites to target de novo muscle development, demonstrating the potential of light-based methods for in situ use [63].

An alternative to in situ printing, which may be limited by a clinician's flexibility and time constraints, is to explore methods for the secure storage of printed tissue scaffolds. In such cases, cryopreservation techniques for "off-the-shelf" bioprinted scaffolds are an interesting solution. Development of a safe, sterile, and effective cryopreservation protocol was demonstrated by Jeon et al. The authors investigated the effects of cryopreservation on MSC-laden OMA microgels and saw no significant differences in DNA content, ALP activity, or GAG content between cryopreserved and fresh microgels, suggesting this technique could be a promising option for translation to clinical use [61]. Other alternatives include the development and storage of acellular scaffolds. Oxford Performance Materials was the first company to obtain FDA 510(k) clearance for 3D-printed patient-specific osseointegrative implants. Their Osteofab technology utilizes polyetherketoneketone (PEKK) polymer fused via selective laser sintering [122]. Clinically integrating additional acellular devices is more feasible due to their reduced complexity and may offer simpler printability by mitigating phototoxicity and other harmful processing-related effects on encapsulated cells.

Although there are no commercialized 3D-bioprinted TERM scaffolds currently available for MSK applications, Vericel Corporation received FDA approval to use patients' own chondrocytes seeded on porcine collagen membranes to culture cellular autologous grafts for repairing cartilage defects [123–125].

Their fabrication strategy does not include 3D printing, but it does demonstrate the advancement of TERM in industry and suggests that a future for bioprinting could be short to follow. Several companies offer commercial resins suitable for 3D bioprinting in research settings. For instance, CELLINK and Advanced Biomatrix provide numerous hydrogel inks, including gelMA-based, collagen-based, HA-based, alginate-based, chitosan-based, dextran-based, and fibrin-based resins, with Irgacure, LAP, and Ru/SPS kit options. Other companies, such as Merck, offer similar materials, including hydrogel kits for tissue-specific dECM, HA, and gelMA. The growing availability of biocompatible and customizable inks is a key factor in enabling more practical and effective applications.

6 | Conclusions

Light-based and nonlight-based printing methods produce constructs with different properties and levels of manufacturing efficiency, with each approach associated with its own set of advantages and limitations. Light-based approaches tend to yield higher resolution structures, which is advantageous for tissues that require fine spatial control. This would be particularly useful in applications such as tissue-on-chip platforms and the development of vascularized tissue scaffolds. These methods enable rapid crosslinking, resulting in shorter fabrication times than alternative biomanufacturing techniques such as freeze-drying or chemical crosslinking. Moreover, photocrosslinking can be combined with secondary crosslinking methods, offering options for increased mechanical stability and a broader range of crosslinking strategies.

As light-assisted bioprinting evolves, addressing the technical, biological, and logistical challenges will be essential for realizing full clinical and industrial potential. The future may see more widespread use of in situ bioprinting technologies, such as the Biopen, to directly print tissues and scaffolds at the point of care, enhancing both the speed and precision of tissue engineering. Regardless, bioprinting will likely require the development of more efficient, cost-effective, and reproducible strategies that provide printed tissues and organs with appropriate safety and functionality. By overcoming these challenges and harnessing ongoing technological advancements, 3D bioprinting may transform musculoskeletal tissue engineering, providing personalized and efficient solutions for tissue repair and regeneration.

Author Contributions

Meagan Morgan: writing – original draft (equal). **Bin Zhang**: writing – original draft (equal). **Roger Narayan**: writing – review & editing (lead).

Funding

The authors received no financial support for the research associated with this article.

Conflicts of Interest

The authors declares no conflicts of interest.

Data Availability Statement

Data availability is not applicable to this article as no datasets were generated or analyzed for this review article.

References

1. P. M. Clark and B. M. Ellis, "A Public Health Approach to Musculoskeletal Health," *Best Practice & Research Clinical Rheumatology* 28, no. 3 (2014): 517–532, https://doi.org/10.1016/j.berh.2014.10.002.

2. A. Yau, K. Yeh, and Y. Chen, "Chapter 10 - Musculoskeletal Tissue Chips," in *Musculoskeletal Tissue Engineering*, eds. Y. Chen (Elsevier, 2022), 275–304, Elsevier Series on Advanced Topics in Biomaterials, https://doi.org/10.1016/B978-0-12-823893-6.00011-5.

3. A. T. Nguyen, I. M. Aris, B. D. Snyder, et al., "Musculoskeletal Health: An Ecological Study Assessing Disease Burden and Research Funding," *The Lancet Regional Health–Americas* 29 (2024): 100661, https://doi.org/10.1016/j.lana.2023.100661.

4. J. T. Huh, J. J. Yoo, A. Atala, and S. J. Lee, "Chapter 74 - Three-Dimensional Bioprinting for Tissue Engineering," in *Principles of Tissue Engineering*, eds. R. Lanza, R. Langer, J. P. Vacanti and A. Atala, 5th ed. (Academic Press, 2020), 1391–1415, https://doi.org/10.1016/B978-0-12-818422-6.00076-9.

5. T. Potyondy, J. Alfredo Uquillas, P. J. Tebon, et al., "Recent Advances in 3D Bioprinting of Musculoskeletal Tissues," *Biofabrication* 13, no. 2 (2021): 022001, https://doi.org/10.1088/1758-5090/abc8de.

6. Our Story, 2017, "3D Systems," Cited April 27, 2026, https://www.3dsystems.com/our-story.

7. G. Lu, R. Tang, J. Nie, and X. Zhu, "Photocuring 3D Printing of Hydrogels: Techniques, Materials, and Applications in Tissue Engineering and Flexible Devices," *Macromolecular Rapid Communications* 45, no. 7 (2024): 2300661, https://doi.org/10.1002/marc.202300661.

8. S. Derakhshanfar, R. Mbeleck, K. Xu, X. Zhang, W. Zhong, and M. Xing, "3D Bioprinting for Biomedical Devices and Tissue Engineering: A Review of Recent Trends and Advances," *Bioactive Materials* 3, no. 2 (2018): 144–156, https://doi.org/10.1016/j.bioactmat.2017.11.008.

9. A. K. Kushwaha, M. H. Rahman, D. Hart, et al., "3 - Fundamentals of Stereolithography: Techniques, Properties, and Applications," *Tribology of Additively Manufactured Materials*, eds. P. Kumar, M. Misra and P. L. Menezes (Elsevier, Elsevier Series on Tribology and Surface Engineering, 2022), 87–106, https://doi.org/10.1016/B978-0-12-821328-5.00003-2.

10. P. Lakkala, S. R. Munnangi, S. Bandari, and M. Repka, "Additive Manufacturing Technologies with Emphasis on Stereolithography 3D Printing in Pharmaceutical and Medical Applications: A Review," *International Journal of Pharmaceutics: X* 5 (2023): 100159, https://doi.org/10.1016/j.ijpx.2023.100159.

11. Y. G. Jeong, J. J. Yoo, S. J. Lee, and M. S. Kim, "3D Digital Light Process Bioprinting: Cutting-Edge Platforms for Resolution of Organ Fabrication," *Materials Today Bio* 29 (2024): 101284, https://doi.org/10.1016/j.mtbio.2024.101284.

12. Y. Jeon, M. Kim, and K. H. Song, "Development of Hydrogels Fabricated via Stereolithography for Bioengineering Applications," *Polymers* 17, no. 6 (2025): 765, https://dpo.org/10.3390/polym17060765.

13. X. Z. Chang, J. S. Liu, and J. Q. Lü, "Digital Light Processing 3D Printing Technology in Biomedical Engineering: A Review," *Macromolecular Bioscience* 25 (2025): 2500101, https://doi.org/10.1002/mabi.202500101.

14. F. A. H. Khalak, J. M. Decuyper, K. A. H. Khalak, S. R. Alonso, L. Saenz-del-Burgo, and J. L. Pedraz Muñoz, "3D Bioprinting

Approaches for Musculoskeletal Interfaces in Tissue Engineering," *International Journal of Pharmaceutics* 682 (2025): 125939, https://doi.org/10.1016/j.ijpharm.2025.125939.

15. E. A. Chiticaru and M. Ioniță, "Commercially Available Bioinks and State-of-the-Art Lab-Made Formulations for Bone Tissue Engineering: A Comprehensive Review," *Materials Today Bio* 29 (2024): 101341, https://doi.org/10.1016/j.mtbio.2024.101341.

16. Y. Lai, X. Xiao, Z. Huang, et al., "Photocrosslinkable Biomaterials for 3D Bioprinting: Mechanisms, Recent Advances, and Future Prospects," *International Journal of Molecular Sciences* 25, no. 23 (2024): 12567, https://doi.org/10.3390/ijms252312567.

17. M. B. Riffe, M. D. Davidson, G. Seymour, et al., "Multi-Material Volumetric Additive Manufacturing of Hydrogels using Gelatin as a Sacrificial Network and 3D Suspension Bath," *Advanced Materials* 36, no. 34 (2024): 2309026, https://doi.org/10.1002/adma.202309026.

18. P. Robles Martinez, A. W. Basit, and S. Gaisford, "Developments and Opportunities of Stereolithography," in *3D Printing of Pharmaceuticals*, eds. A. W. Basit and S. Gaisford (Springer International Publishing, 2018), 55–79, https://doi.org/10.1007/978-3-319-90755-0_4.

19. J. M. Lee, W. L. Ng, and W. Y. Yeong, "Resolution and Shape in Bioprinting: Strategizing towards Complex Tissue and Organ Printing," *Applied Physics Reviews* 6, no. 1 (2019): 011307, https://doi.org/10.1063/1.5053909.

20. A. K. Miri, I. Mirzaee, S. Hassan, et al., "Effective Bioprinting Resolution in Tissue Model Fabrication," *Lab on a Chip* 19, no. 11 (2019): 2019–2037, https://doi.org/10.1039/C8LC01037D.

21. Y. Bao, "Recent Trends in Advanced Photoinitiators for Vat Photopolymerization 3D Printing," *Macromolecular Rapid Communications* 43, no. 14 (2022): 2200202, https://doi.org/10.1002/marc.202200202.

22. J. F. Xing, M. L. Zheng, and X. M. Duan, "Two-Photon Polymerization Microfabrication of Hydrogels: An Advanced 3D Printing Technology for Tissue Engineering and Drug Delivery," *Chemical Society Reviews* 44, no. 15 (2015): 5031–5039, https://doi.org/10.1039/C5CS00278H.

23. H. Kavand, H. van Lintel, S. Bakhshi Sichani, et al., "Cell-Imprint Surface Modification by Contact Photolithography-Based Approaches: Direct-Cell Photolithography and Optical Soft Lithography Using PDMS Cell Imprints," *ACS Applied Materials & Interfaces* 11, no. 11 (2019): 10559–10566, https://doi.org/10.1021/acsami.9b00523.

24. D. Loterie, P. Delrot, and C. Moser, "High-Resolution Tomographic Volumetric Additive Manufacturing," *Nature Communications* 11 (2020): 852, https://doi.org/10.1038/s41467-020-14630-4.

25. C. D. Amo, M. Perez-Garrastachu, I. Jauregui, X. Llama-Pino, and I. Andia, "Assessing Bioprinted Functionalized Grafts for Biological Tendon Augmentation In Vitro," *International Journal of Molecular Sciences* 25, no. 9 (2024): 4752, https://doi.org/10.3390/ijms25094752.

26. M. Setayeshmehr, S. Hafeez, C. van Blitterswijk, L. Moroni, C. Mota, and M. B. Baker, "Bioprinting Via a Dual-Gel Bioink Based on Poly(Vinyl Alcohol) and Solubilized Extracellular Matrix towards Cartilage Engineering," *International Journal of Molecular Sciences* 22, no. 8 (2021): 3901, https://doi.org/10.3390/ijms22083901.

27. S.-L. Chen, M. Senadeera, K. Ruberu, et al., "Machine Learning-Generated Compression Modulus Database for 3D Printing of Gelatin Methacryloyl," *International Journal of Bioprinting* 10, no. 5 (2024): 3814, https://doi.org/10.36922/ijb.3814.

28. Y. Chu, L. Huang, W. Hao, et al., "Long-Term Stability, High Strength, and 3D Printable Alginate Hydrogel for Cartilage Tissue Engineering Application," *Biomedical Materials* 16, no. 6 (2021): 064102, https://doi.org/10.1088/1748-605X/ac2595.

29. J. H. Galarraga, M. Y. Kwon, and J. A. Burdick, "3D Bioprinting via an In Situ Crosslinking Technique towards Engineering Cartilage Tissue," *Scientific Reports* 9 (2019): 19987, https://doi.org/10.1038/s41598-019-56117-3.

30. J. S. Lee, H. Jung, O. Ajiteru, et al., "Hybrid 3D Bioprinting for Advanced Tissue-Engineered Trachea: Merging Fused Deposition Modeling (FDM) and Top-Down Digital Light Processing (DLP)," *Biofabrication* 17, no. 1 (2024): 015026, https://doi.org/10.1088/1758-5090/ad92da.

31. S. Zhu, Z. Zhou, X. Chen, et al., "High Mechanical Performance and Multifunctional Degraded Fucoidan-Derived Bioink for 3D Bioprinting," *Carbohydrate Polymers* 348 (2025): 122805, https://doi.org/10.1016/j.carbpol.2024.122805.

32. F. Wulle, O. Gorke, S. Schmidt, et al., "Multi-Axis 3D Printing of Gelatin Methacryloyl Hydrogels on a Non-Planar Surface Obtained from Magnetic Resonance Imaging," *Additive Manufacturing* 50 (2022): 102566, https://doi.org/10.1016/j.addma.2021.102566.

33. A. Almalla, L. Elomaa, N. Fribiczer, et al., "Chemistry Matters: A Side-by-Side Comparison of Two Chemically Distinct Methacryloylated dECM Bioresins for Vat Photopolymerization," *Biomaterials Advances* 160 (2024): 213850, https://doi.org/10.1016/j.bioadv.2024.213850.

34. W. Kiratitanaporn, D. B. Berry, A. Mudla, et al., "3D Printing a Biocompatible Elastomer for Modeling Muscle Regeneration after Volumetric Muscle Loss," *Biomaterials Advances* 142 (2022): 213171, https://doi.org/10.1016/j.bioadv.2022.213171.

35. M. Hospodiuk, M. Dey, D. Sosnoski, and I. T. Ozbolat, "The Bioink: A Comprehensive Review on Bioprintable Materials," *Biotechnology Advances* 35, no. 2 (2017): 217–239, https://doi.org/10.1016/j.biotechadv.2016.12.006.

36. W. Jia, Z. Liu, L. Sun, et al., "A Multicrosslinked Network Composite Hydrogel Scaffold Based on DLP Photocuring Printing for Nasal Cartilage Repair," *Biotechnology and Bioengineering* 121, no. 9 (2024): 2752–2766, https://doi.org/10.1002/bit.28769.

37. K. S. Lim, J. H. Galarraga, X. Cui, G. C. J. Lindberg, J. A. Burdick, and T. B. F. Woodfield, "Fundamentals and Applications of Photo-Cross-Linking in Bioprinting," *Chemical Reviews* 120, no. 19 (2020): 10662–10694, https://doi.org/10.1021/acs.chemrev.9b00812.

38. K. S. Lim, F. Abinzano, P. N. ñez Bernal, et al., "One-Step Photoactivation of a Dual-Functionalized Bioink as Cell Carrier and Cartilage-Binding Glue for Chondral Regeneration," *Advanced Healthcare Materials* 9, no. 15 (2020): e1901792, https://doi.org/10.1002/adhm.201901792.

39. H. Liang, Y. Wang, S. Chen, Y. Liu, Z. Liu, and J. Bai, "Nano-Hydroxyapatite Bone Scaffolds with Different Porous Structures Processed by Digital Light Processing 3D Printing," *International Journal of Bioprinting* 8, no. 1 (2022): 502. https://doi.org/10.18063/ijb.v8i1.502.

40. M. L. Bedell, A. L. Torres, K. J. Hogan, et al., "Human Gelatin-Based Composite Hydrogels for Osteochondral Tissue Engineering and Their Adaptation into Bioinks for Extrusion, Inkjet, and Digital Light Processing Bioprinting," *Biofabrication* 14, no. 4 (2022): 045012, https://doi.org/10.1088/1758-5090/ac8768.

41. J. Huh, Y. W. Moon, J. Park, A. Atala, J. J. Yoo, and S. J. Lee, "Combinations of Photoinitiator and UV Absorber for Cell-Based Digital Light Processing (DLP) Bioprinting," *Biofabrication* 13, no. 3 (2021): 034103, https://doi.org/10.1088/1758-5090/abfd7a.

42. C. Xie, R. Liang, J. Ye, et al., "High-Efficient Engineering of Osteo-Callus Organoids for Rapid Bone Regeneration Within 1 Month," *Biomaterials* 288 (2022): 121741, https://doi.org/10.1016/j.biomaterials.2022.121741.

43. X. Xie, S. Wu, S. Mou, N. Guo, Z. Wang, and J. Sun, "Microtissue-Based Bioink as a Chondrocyte Microshelter for DLP Bioprinting," *Advanced Healthcare Materials* 11, no. 22 (2022): 2201877, https://doi.org/10.1002/adhm.202201877.

44. X. Ren, J. Wang, Y. Wu, et al., "One-Pot Synthesis of Hydroxyapatite Hybrid Bioinks for Digital Light Processing 3D Printing in Bone Regeneration," *Journal of Materials Science & Technology* 188 (2024): 84–97, https://doi.org/10.1016/j.jmst.2024.01.001.

45. L. Zhou, D. Chen, R. Wu, et al., "An Injectable and Photocurable Methacrylate-Silk Fibroin/Nano-Hydroxyapatite Hydrogel for Bone Regeneration through Osteoimmunomodulation," *International Journal of Biological Macromolecules* 263, no. Pt 1 (2024): 129925, https://doi.org/10.1016/j.ijbiomac.2024.129925.

46. J. Sun, J. Binner, and J. Bai, "Effect of Surface Treatment on the Dispersion of Nano Zirconia Particles in Non-Aqueous Suspensions for Stereolithography," *Journal of the European Ceramic Society* 39, no. 4 (2019): 1660–1667, https://doi.org/10.1016/j.jeurceramsoc.2018.10.024.

47. M. Zhao, H. Liu, X. Zhang, and J. Qin, "Advances in Skeletal Muscle Engineering in Biomedical Research," *Advanced Materials Technologies* 8, no. 22 (2023): 2300595, https://doi.org/10.1002/admt.202300595.

48. Y. X. Wang and M. A. Rudnicki, "Satellite Cells, the Engines of Muscle Repair," *Nature Reviews Molecular Cell Biology* 13, no. 2 (2012): 127–133, https://doi.org/10.1038/nrm3265.

49. B. T. Corona, K. Garg, C. L. Ward, J. S. McDaniel, T. J. Walters, and C. R. Rathbone, "Autologous Minced Muscle Grafts: A Tissue Engineering Therapy for the Volumetric Loss of Skeletal Muscle," *American Journal of Physiology-Cell Physiology* 305, no. 7 (2013): C761–C775, https://doi.org/10.1152/ajpcell.00189.2013.

50. J. Tao, S. Zhu, N. Zhou, et al., "Nanoparticle-Stabilized Emulsion Bioink for Digital Light Processing Based 3D Bioprinting of Porous Tissue Constructs," *Advanced Healthcare Materials* 11, no. 12 (2022): 2102810, https://doi.org/10.1002/adhm.202102810.

51. L. K. Shopperly, J. Spinnen, J. Philipp Krüger, et al., "Blends of Gelatin and Hyaluronic Acid Stratified by Stereolithographic Bioprinting Approximate Cartilaginous Matrix Gradients," *Journal of Biomedical Materials Research Part B: Applied Biomaterials* 110, no. 10 (2022): 2310–2322, https://doi.org/10.1002/jbm.b.35079.

52. J. Shen, W. Song, J. Liu, et al., "3D Bioprinting by Reinforced Bioink Based on Photocurable Interpenetrating Networks for Cartilage Tissue Engineering," *International Journal of Biological Macromolecules* 254 (2024): 127671, https://doi.org/10.1016/j.ijbiomac.2023.127671.

53. A. Puiggalí-Jou, R. Rizzo, A. Bonato, et al., "FLight Biofabrication Supports Maturation of Articular Cartilage with Anisotropic Properties," *Advanced Healthcare Materials* 13, no. 12 (2024): 2302179, https://doi.org/10.1002/adhm.202302179.

54. Y. Huang, X. Meng, Z. Zhou, et al., "A Naringin-Derived Bioink Enhances the Shape Fidelity of 3D Bioprinting and Efficiency of Cartilage Defect Repair," *Journal of Materials Chemistry B* 10, no. 36 (2022): 7030–7044, https://doi.org/10.1039/D2TB01247B.

55. S. H. Kim, Y. B. Seo, Y. K. Yeon, et al., "4D-Bioprinted Silk Hydrogels for Tissue Engineering," *Biomaterials* 260 (2020): 120281, https://doi.org/10.1016/j.biomaterials.2020.120281.

56. E. Senturk, C. Bilici, F. Afghah, et al., "3D Bioprinting of Tyramine Modified Hydrogels under Visible Light for Osteochondral Interface," *Biofabrication* 15, no. 3 (2023): 034102, https://doi.org/10.1088/1758-5090/acd6bf.

57. K. Behan, A. Dufour, O. Garcia, and D. Kelly, "Methacrylated Cartilage ECM-Based Hydrogels as Injectables and Bioinks for Cartilage Tissue Engineering," *Biomolecules* 12, no. 2 (2022): 216, https://doi.org/10.3390/biom12020216.

58. A. K. X. Lee, Y. H. Lin, C. H. Tsai, W. T. Chang, T. L. Lin, and M. Y. Shie, "Digital Light Processing Bioprinted Human Chondrocyte-Laden Poly (γ-Glutamic Acid)/Hyaluronic Acid Bio-Ink towards Cartilage Tissue Engineering," *Biomedicines* 9, no. 7 (2021): 714, https://doi.org/10.3390/biomedicines9070714.

59. G. Irmak and M. Gümüşderelioğlu, "Photo-Activated Platelet-Rich Plasma (PRP)-Based Patient-Specific Bio-Ink for Cartilage Tissue Engineering," *Biomedical Materials* 15, no. 6 (2020): 065010, https://doi.org/10.1088/1748-605X/ab9e46.

60. C. Luo, R. Xie, J. Zhang, et al., "Low-Temperature Three-Dimensional Printing of Tissue Cartilage Engineered with Gelatin Methacrylamide," *Tissue Engineering Part C: Methods* 26, no. 6 (2020): 306–316, https://doi.org/10.1089/ten.tec.2020.0053.

61. O. Jeon, Y. B. Lee, T. J. Hinton, A. W. Feinberg, and E. Alsberg, "Cryopreserved Cell-Laden Alginate Microgel Bioink for 3D Bioprinting of Living Tissues," *Materials Today Chemistry* 12 (2019): 61–70, https://doi.org/10.1016/j.mtchem.2018.11.009.

62. A. I. Frías-Sánchez, D. A. Quevedo-Moreno, M. Samandari, et al., "Biofabrication of Muscle Fibers Enhanced with Plant Viral Nanoparticles Using Surface Chaotic Flows," *Biofabrication* 13, no. 3 (2021): 035015, https://doi.org/10.1088/1758-5090/abd9d7.

63. A. Urciuolo, I. Poli, L. Brandolino, et al., "Intravital Three-Dimensional Bioprinting," *Nature Biomedical Engineering* 4, no. 9 (2020): 901–915, https://doi.org/10.1038/s41551-020-0568-z.

64. F. L. Ronzoni, F. Aliberti, F. Scocozza, et al., "Myoblast 3D Bioprinting to Burst In Vitro Skeletal Muscle Differentiation," *Journal of Tissue Engineering and Regenerative Medicine* 16, no. 5 (2022): 484–495, https://doi.org/10.1002/term.3293.

65. R. Seyedmahmoud, B. Çelebi-Saltik, N. Barros, et al., "Three-Dimensional Bioprinting of Functional Skeletal Muscle Tissue Using Gelatin Methacryloyl-Alginate Bioinks," *Micromachines* 10, no. 10 (2019): 10, https://doi.org/10.3390/mi10100679.

66. B. Sanz, A. Albillos Sanchez, B. Tangey, et al., "Light Cross-Linkable Marine Collagen for Coaxial Printing of a 3D Model of Neuromuscular Junction Formation," *Biomedicines* 9, no. 1 (2020): 16, https://doi.og/10.3390/biomedicines9010016.

67. Y. Ma, X. Yang, Y. Chen, et al., "Biomimetic Peridontium Patches for Functional Periodontal Regeneration," *Advanced Healthcare Materials* 12, no. 7 (2023): 2202169, https://doi.org/10.1002/adhm.202202169.

68. M. Rajput, P. Mondal, P. Yadav, and K. Chatterjee, "Light-Based 3D Bioprinting of Bone Tissue Scaffolds with Tunable Mechanical Properties and Architecture from Photocurable Silk Fibroin," *International Journal of Biological Macromolecules* 202 (2022): 644–656, https://doi.org/10.1016/j.ijbiomac.2022.01.081.

69. J. Tao, S. Zhu, X. Liao, et al., "DLP-Based Bioprinting of Void-Forming Hydrogels for Enhanced Stem-Cell-Mediated Bone Regeneration," *Materials Today Bio* 17 (2022): 100487, https://doi.org/10.1016/j.mtbio.2022.100487.

70. M. Wang, W. Li, L. S. Mille, et al., "Digital Light Processing Based Bioprinting with Composable Gradients," *Advanced Materials* 34, no. 1 (2022): 2107038, https://doi.org/10.1002/adma.202107038.

71. J. Gehlen, W. Qiu, G. N. Schadli, R. Mueller, and X. H. Qin, "Tomographic Volumetric Bioprinting of Heterocellular Bone-Like Tissues in Seconds," *Acta Biomaterialia* 156 (2023): 49–60, https://doi.org/10.1016/j.actbio.2022.06.020.

72. M. Yang, L. Chu, Y. Zhuang, et al., "Multi-Material Digital Light Processing (DLP) Bioprinting of Heterogeneous Hydrogel Constructs with Perfusable Networks," *Advanced Functional Materials* 34, no. 32 (2024): 2316456, https://doi.org/10.1002/adfm.202316456.

73. H. Shi, Y. Li, K. Xu, and J. Yin, "Advantages of Photo-Curable Collagen-Based Cell-Laden Bioinks Compared to Methacrylated Gelatin (GelMA) in Digital Light Processing (DLP) and Extrusion Bioprinting," *Materials Today Bio* 23 (2023): 100799, https://doi.org/10.1016/j.mtbio.2023.100799.

74. J. Gao, H. Wang, M. Li, et al., "DLP-Printed GelMA-PMAA Scaffold for Bone Regeneration through Endochondral Ossification," *International Journal of Bioprinting* 9, no. 5 (2023): 754, https://doi.org/10.18063/ijb.754.

75. S. Kumari, P. Mondal, S. Tyeb, and K. Chatterjee, "Visible Light-Based 3D Bioprinted Composite Scaffolds of κ-Carrageenan for Bone Tissue Engineering Applications," *Journal of Materials Chemistry B* 12, no. 7 (2024): 1926–1936, https://doi.org/10.1039/d3tb02179c.

76. A. Bucciarelli, M. Petretta, B. Grigolo, et al., "Methacrylated Silk Fibroin Additive Manufacturing of Shape Memory Constructs with Possible Application in Bone Regeneration," *Gels* 8, no. 12 (2022): 833, https://doi.org/10.3390/gels8120833.

77. S. C. Marks and P. R. Odgren, "Chapter 1 - Structure and Development of the Skeleton," *Principles of Bone Biology*, eds. J. P. Bilezikian, L. G. Raisz, and G. A. Rodan, 2nd ed. (Academic Press, 2002), 3–15, https://doi.org/10.1016/B978-012098652-1.50103-7.

78. B. Clarke, "Normal Bone Anatomy and Physiology," *Clinical Journal of the American Society of Nephrology* 3, no. S3 (2008): S131–S139, https://doi.org/10.2215/CJN.04151206.

79. V. Šromová, D. Sobola, and P. Kaspar, "A Brief Review of Bone Cell Function and Importance," *Cells* 12, no. 21 (2023): 2576, https://doi.org/10.3390/cells12212576.

80. A. Wawrzyniak and K. Balawender, "Structural and Metabolic Changes in Bone," *Animals* 12, no. 15 (2022): 1946, https://doi.org/10.3390/ani12151946.

81. Z. Mackiewicz, W. E. Niklińska, J. Kowalewska, and L. Chyczewski, "Bone as a Source of Organism Vitality and Regeneration," *Folia Histochemica Et Cytobiologica* 49, no. 4 (2011): 558–569, https://doi.org/10.5603/fhc.2011.0079.

82. S. Bolamperti, I. Villa, and A. Rubinacci, "Bone Remodeling: An Operational Process Ensuring Survival and Bone Mechanical Competence," *Bone Research* 10, no. 1 (2022): 1–19, https://doi.org/10.1038/s41413-022-00219-8.

83. H. Yuan and W. Cui, "The Lubricated Matter in Body," *Progress in Materials Science* 146 (2024): 101334, https://doi.org/10.1016/j.pmatsci.2024.101334.

84. P. Gerdhem, "Osteoporosis and Fragility Fractures: Vertebral Fractures," *Best Practice & Research Clinical Rheumatology* 27, no. 6 (2013): 743–755, https://doi.org/10.1016/j.berh.2014.01.002.

85. G. Li, J. Yin, J. Gao, et al., "Subchondral Bone in Osteoarthritis: Insight into Risk Factors and Microstructural Changes," *Arthritis Research & Therapy* 15, no. 6 (2013): 223, https://doi.org/10.1186/ar4405.

86. G. Chindamo, S. Sapino, E. Peira, D. Chirio, M. C. Gonzalez, and M. Gallarate, "Bone Diseases: Current Approach and Future Perspectives in Drug Delivery Systems for Bone Targeted Therapeutics," *Nanomaterials* 10, no. 5 (2020): 875, https://doi.org/10.3390/nano10050875.

87. S. Alharbi, "A Systematic Overview of Osteogenesis Imperfecta," *Molecular Biology* 05, no. 01 (2015): 1–9, https://doi.org/10.4172/2168-9547.1000150.

88. A. Sculean, A. Stavropoulos, and D. D. Bosshardt, "Self-Regenerative Capacity of Intra-Oral Bone Defects," *Journal of Clinical Periodontology* 46 (2019): 70–81, https://doi.org/10.1111/jcpe.13075.

89. J. J. Li, M. Ebied, J. Xu, and H. Zreiqat, "Current Approaches to Bone Tissue Engineering: The Interface between Biology and Engineering," *Advanced Healthcare Materials* 7, no. 6 (2018): 1701061, https://doi.org/10.1002/adhm.201701061.

90. M. Altunbek, S. F. Afghah, A. Fallah, A. A. Acar, and B. Koc, "Design and 3D Printing of Personalized Hybrid and Gradient Structures for Critical Size Bone Defects," *ACS Applied Bio Materials* 6, no. 5 (2023): 1873–1885, https://doi.org/10.1021/acsabm.3c00107.

91. B. Zhang, S. H. Chung, S. Barker, D. Craig, R. J. Narayan, and J. Huang, "Direct Ink Writing of Polycaprolactone/Polyethylene Oxide Based 3D Constructs," *Progress in Natural Science: Materials International* 31, no. 2 (2021): 180–191, https://doi.org/10.1016/j.pnsc.2020.10.001.

92. B. Zhang, J. Huang, and R. J. Narayan, "Gradient Scaffolds for Osteochondral Tissue Engineering and Regeneration," *Journal of Materials Chemistry B* 8, no. 36 (2020): 8149–8170, https://doi.org/10.1039/D0TB00688B.

93. M. Ge, D. Xie, C. Jiao, et al., "Mechanical Properties and Biocompatibility of MgO/Ca3(PO4)2 Composite Ceramic Scaffold with High MgO Content Based on Digital Light Processing," *Ceramics International* 48, no. 15 (2022): 21175–21186, https://doi.org/10.1016/j.ceramint.2022.04.010.

94. H. Zhang, C. Jiao, Z. Liu, et al., "3D-Printed Composite, Calcium Silicate Ceramic Doped with CaSO4·2H2O: Degradation Performance and Biocompatibility," *Journal of the Mechanical Behavior of Biomedical Materials* 121 (2021): 104642, https://doi.org/10.1016/j.jmbbm.2021.104642.

95. N. Nasiri, S. Taheri, S. Hosseini, and M. Baghaban Eslaminejad, "Introduction to Cartilage Tissue: Development, Structure, and Functions," in *Cartilage: From Biology to Biofabrication*, eds. M. Baghaban Eslaminejad and S. Hosseini (Springer Nature, 2023), 1–20, https://doi.org/10.1007/978-981-99-2452-3_1.

96. M. Müller, E. Öztürk, Ø. Arlov, P. Gatenholm, and M. Zenobi-Wong, "Alginate Sulfate–Nanocellulose Bioinks for Cartilage Bioprinting Applications," *Annals of Biomedical Engineering* 45, no. 1 (2017): 210–223, https://doi.org/10.1007/s10439-016-1704-5.

97. K. Zhang, Q. Feng, J. Xu, et al., "Self-Assembled Injectable Nanocomposite Hydrogels Stabilized by Bisphosphonate-Magnesium (Mg2+) Coordination Regulates the Differentiation of Encapsulated Stem Cells via Dual Crosslinking," *Advanced Functional Materials* 27, no. 34 (2017): 1701642, https://doi.org/10.1002/adfm.201701642.

98. K. H. Yang, G. Lindberg, B. Soliman, K. Lim, T. Woodfield, and R. J. Narayan, "Effect of Photoinitiator on Precursory Stability and Curing Depth of Thiol-Ene Clickable Gelatin," *Polymers* 13, no. 11 (2021): 1877, https://doi.org/10.3390/polym13111877.

99. K. S. Lim, B. J. Klotz, G. C. J. Lindberg, et al., "Visible Light Cross-Linking of Gelatin Hydrogels Offers an Enhanced Cell Microenvironment with Improved Light Penetration Depth," *Macromolecular Bioscience* 19, no. 6 (2019): 1900098, https://doi.org/10.1002/mabi.201900098.

100. A. J. Capel, R. P. Rimington, J. W. Fleming, et al., "Scalable 3D Printed Molds for Human Tissue Engineered Skeletal Muscle," *Frontiers in Bioengineering and Biotechnology* 7 (2019): 20, https://doi.org/10.3389/fbioe.2019.00020.

101. R. Mestre, T. Patiño, X. Barceló, S. Anand, A. Pérez-Jiménez, and S. Sánchez, "Force Modulation and Adaptability of 3D-Bioprinted Biological Actuators Based on Skeletal Muscle Tissue," *Advanced Materials Technologies* 4, no. 2 (2019): 1800631, https://doi.org/10.1002/admt.201800631.

102. M. Javan Almasi and D. Xiong, "Recent Progress in Bionic Hydrogels for Articular Cartilage: Tribological and Mechanical Characteristics," *Journal of Bionic Engineering* 21, no. 2 (2024): 653–673, https://doi.org/10.1007/s42235-024-00480-z.

103. P. Chansoria, S. Asif, N. Gupta, J. Piedrahita, and R. A. Shirwaiker, "Multiscale Anisotropic Tissue Biofabrication via Bulk Acoustic Patterning of Cells and Functional Additives in Hybrid Bioinks," *Advanced Healthcare Materials* 11, no. 10 (2022): e2102351, https://doi.org/10.1002/adhm.202102351.

104. B. J. Winn, D. J. Haight, D. S. B. Williams, and B. S. Kirby, "Skeletal Muscle Elastic Modulus in Marathon Distance Runners," *European Journal of Applied Physiology* 125, no. 6 (2025): 1701–1715, https://doi.org/10.1007/s00421-025-05708-2.

105. Y. Liu, Y. Wan, C. Li, et al., "Gradient Scaffolds in Bone-Soft Tissue Interface Engineering: Structural Characteristics, Fabrication Techniques, and Emerging Trends," *Journal of Orthopaedic Translation* 50 (2025): 333–353, https://doi.org/10.1016/j.jot.2024.10.015.

106. N. Broguiere, E. Cavalli, G. M. Salzmann, L. A. Applegate, and M. Zenobi-Wong, "Cross-Linked Hyaluronan Hydrogels for Cartilage Tissue Engineering," *ACS Biomaterials Science & Engineering* 2, no. 12 (2016): 2176–2184, https://doi.org/10.1021/acsbiomaterials.6b00378.

107. J. Zhang, E. Wehrle, P. Adamek, et al., "Optimization of Mechanical Stiffness and Cell Density of 3D Bioprinted Cell-Laden Scaffolds Improves Extracellular Matrix Mineralization and Cellular Organization for Bone Tissue Engineering," *Acta Biomaterialia* 114 (2020): 307–322, https://doi.org/10.1016/j.actbio.2020.07.016.

108. R. G. M. Breuls, T. U. Jiya, and T. H. Smit, "Scaffold Stiffness Influences Cell Behavior: Opportunities for Skeletal Tissue Engineering," *The Open Orthopaedics Journal* 2 (2008): 103–109, https://doi.org/10.2174/1874325000802010103.

109. J. Toombs, C. C. Li, N. Akiki, Y. Sun, and H. Taylor, "Roll-to-Roll Tomographic Volumetric Additive Manufacturing," *arXiv preprint*. (2024), arXiv:2402.10955 https://doi.org/10.48550/arXiv.2402.10955.

110. L. Stüwe, M. Geiger, F. Röllgen, et al., "Continuous Volumetric 3D Printing: Xolography in Flow," *Advanced Materials* 36, no. 4 (2024): 2306716, https://doi.org/10.1002/adma.202306716.

111. K. S. Lim, M. Baptista, S. Moon, T. B. F. Woodfield, and J. Rnjak-Kovacina, "Microchannels in Development, Survival, and Vascularisation of Tissue Analogues for Regenerative Medicine," *Trends in Biotechnology* 37, no. 11 (2019): 1189–1201, https://doi.org/10.1016/j.tibtech.2019.04.004.

112. W. Li, M. Wang, H. Ma, F. A. Chapa-Villarreal, A. O. Lobo, and Y. S. Zhang, "Stereolithography Apparatus and Digital Light Processing-Based 3D Bioprinting for Tissue Fabrication," *IScience* 26, no. 2 (2023): 106039, https://doi.org/10.1016/j.isci.2023.106039.

113. N. Torras, J. Zabalo, E. Abril, A. Carré, M. García-Díaz, and E. Martínez, "A Simple DLP-Bioprinting Strategy Produces Cell-Laden Crypt-Villous Structures for an Advanced 3D Gut Model," *bioRxiv* 5 (2022): 2022.02.09.479715, https://doi.org/10.1101/2022.02.09.479715.

114. G. H. Yang, W. Kim, J. Kim, and G. Kim, "A Skeleton Muscle Model Using GelMA-Based Cell-Aligned Bioink Processed with an Electric-Field Assisted 3D/4D Bioprinting," *Theranostics* 11, no. 1 (2021): 48–63, https://doi.org/10.7150/thno.50794.

115. X. Wu, W. Shi, X. Liu, and Z. Gu, "Recent Advances in 3D-Printing-Based Organ-on-a-Chip," *EngMedicine* 1, no. 1 (2024): 100003, https://doi.org/10.1016/j.engmed.2024.100003.

116. J. Harberts, C. Fendler, J. Teuber, et al., "Toward Brain-on-a-Chip: Human Induced Pluripotent Stem Cell-Derived Guided Neuronal Networks in Tailor-Made 3D Nanoprinted Microscaffolds," *ACS Nano* 14, no. 10 (2020): 13091–13102, https://doi.org/10.1021/acsnano.0c04640.

117. P. N. Bernal, S. Florczak, S. Inacker, et al., "The Road Ahead in Materials and Technologies for Volumetric 3D Printing," *Nature Reviews Materials* 10 (2025): 826–841, https://doi.org/10.1038/s41578-025-00785-3.

118. N. B. Allen, B. Abar, L. Johnson, J. Burbano, R. M. Danilkowicz, and S. B. Adams, "3D-Bioprinted GelMA-Gelatin-Hydroxyapatite Osteoblast-Laden Composite Hydrogels for Bone Tissue Engineering," *Bioprinting* 26 (2022): e00196, https://doi.org/10.1016/j.bprint.2022.e00196.

119. N. S. Kajave, T. Schmitt, T. U. Nguyen, A. K. Gaharwar, and V. Kishore, "Bioglass Incorporated Methacrylated Collagen Bioactive Ink for 3D Printing of Bone Tissue," *Biomedical Materials* 16, no. 3 (2021): 035003, https://doi.org/10.1088/1748-605X/abc744.

120. C. Alparslan and Ş. Bayraktar, "Advances in Digital Light Processing (DLP) Bioprinting: A Review of Biomaterials and Its Applications, Innovations, Challenges, and Future Perspectives," *Polymers* 17, no. 9 (2025): 1287, https://doi.org/10.3390/polym17091287.

121. Y. L. Han, J. Hu, G. M. Genin, T. J. Lu, and F. Xu, "BioPen: Direct Writing of Functional Materials at the Point of Care," *Scientific Reports* 4, no. 1 (2014): 4872, https://doi.org/10.1038/srep04872.

122. A. Maandi, J. Porteus, and B. Roberts, "OsteoFab® Technology" Young 3 (2020): 3–10.

123. M. Brittberg, D. Recker, J. Ilgenfritz, D. B. F. Saris, and SUMMIT Extension Study Group, "Matrix-Applied Characterized Autologous Cultured Chondrocytes Versus Microfracture: Five-Year Follow-up of a Prospective Randomized Trial," *The American Journal of Sports Medicine* 46, no. 6 (2018): 1343–1351, https://doi.org/10.1177/0363546518756976.

124. D. Saris, A. Price, W. Widuchowski, et al., "Matrix-Applied Characterized Autologous Cultured Chondrocytes Versus Microfracture: Two-Year Follow-up of a Prospective Randomized Trial," *The American Journal of Sports Medicine* 42, no. 6 (2014): 1384–1394, https://doi.org/10.1177/0363546514528093.

125. U.S. Food and Drug Administration, "Approved Products: MACI (Autologous Cultured Chondrocytes on a Porcine Collagen Membrane)," (FDA, 2016).

Supporting Information

Additional supporting information can be found online in the Supporting Information section.